Received: 6 March 2020 | Revised: 24 November 2020 | Accepted: 25 November 2020

DOI: 10.1002/ldr.3839

RESEARCH ARTICLE

WILEY

Evaluation of wind erosion control practices at a photovoltaic power station within a sandy area of northwest, China

Chun Wang[1,5] | Robert L. Hill[2] | Chongfeng Bu[1,3] | Bingyin Li[1] | Fang Yuan[1] | Yanzhe Yang[3] | Senpeng Yuan[1] | Zhenshi Zhang[4] | Yongxiang Cao[4] | Kankan Zhang[5]

[1]Institute of Soil and Water Conservation, Northwest A & F University, Yangling, PR China

[2]Department of Environmental Science and Technology, University of Maryland, College Park, Maryland

[3]Institute of Soil and Water Conservation, Chinese Academy of Sciences and Ministry of Water Resources, Yangling, PR China

[4]Urban rural development & environmental protection engineering div, Northwest Engineering Corporation Limited of Power China, Xi'an, PR China

[5]Engineering department, Shaanxi Lvtuo Eco-environment Engineering Co., Ltd, Yangling, PR China

Correspondence
Chongfeng Bu, Northwest A&F University, Institute of Soil and Water Conservation, Xinong Road, No.26, Yangling 712100, Shaanxi, PR China.
Email: buchongfeng@163.com

Funding information
National Key Research and Development Program of China, Grant/Award Numbers: 2016YFE0203400, 2017YFC0504703; the Major Project of Collaborative Innovation of Yangling District, Grant/Award Number: 2017CXY-08; the National Natural Scientific Foundation of China, Grant/Award Number: 41971131; the Northwest Engineering Corporation Limited of Power China Fund; the USDA National Institute of Food and Agriculture, Grant/Award Number: 1014496

Abstract

The widespread construction of photovoltaic power stations within northwest China poses an environmental threat because of severe increased wind erosion and land degradation. Engineering, plant, and biocrust treatments were evaluated in this study for their effectiveness in the reduction of wind erosion. The placement of solar panels caused wind speed variation and resulted in distinct abrasion and deposition zones between the rows of the solar panels and the formation of deflation zones under the solar panels. Combined treatments (gravel and red clay mulch were applied within the abrasion and deposition zones, respectively) and moss-crust were the optimal choices within the engineering and biocrust treatments, respectively. We found that for engineering treatments, the combined procedures led to treatments had sand transport rate reductions of 87%, while the straw checkerboard, gravel, and red clay treatments gave reductions of 51, 78, and 74%, respectively. Within the biocrust treatments, the moss-crust decreased the sand transport rates and the sand erosion–deposit budget by 71 and 114%, respectively, while the cyanobacteria crust caused reductions of 65 and 109%, respectively, in comparison to the control. Both plant treatments decreased the sand transport rates and the sand erosion–deposit budgets, but were inferior to other optimal treatments with the best plant treatment dependent on the placement pattern used for plant establishment. All the treatments had effects on reducing wind erosion, and we strongly recommend the use of moss-crust and combined treatments in the deflation zones and between the rows of the solar panels, respectively, to significantly reduce the severe wind erosion occurring at these photovoltaic power stations located in sandy areas.

KEYWORDS
abrasion, biocrust, deposition, photovoltaic power station, wind erosion control

1 | INTRODUCTION

Twenty-five percent of the Earth's land area is affected by land degradation that gives rise to a series of negative ecological and economic consequences, such as reductions in ecosystem services and the corresponding degradation of ecosystem goods, increased soil losses, water quality deterioration, reduced biodiversity, and reductions in food production (Pacheco, Sanches Fernandes, Valle Junior, Valera, & Pissarra, 2018). Ecosystem function impairments attributed to land degradation have caused average annual global losses of US$ 6.3 trillion in ecosystem service values (Sutton, Anderson, Costanza, & Kubiszewski, 2016). These losses stress the importance of restoring

degraded lands and preventing the degradation of additional lands. Zero net land degradation (land degradation neutrality, LDN) was developed as a target by the United Nations Convention to Combat Desertification (UNCCD) (Chasek et al., 2019; Gilbey, Davies, Metternicht, & Magero, 2019; Sutton et al., 2016).

Wind erosion is a major contributor to land degradation with one-third of the global terrestrial land areas impacted by wind erosion (Giménez, Lozano, Torres, & Asensio, 2019; Zhang et al., 2018). Wind erosion interacts directly with the topsoil, where it removes fine particles and depletes associated nutrients, changes soil texture and soil particle size distribution, decreases nutrient and organic matter contents, and amplifies the rate of water evaporation (Li, Okin, & Epstein, 2009; Wang, Guo, Chang, Xiao, & Jiang, 2015; Yan et al., 2013). These changes reduce the soil's susceptibility to erosion and increase the potential for additional soil degradation. Therefore, effectively reducing wind erosion can help mitigate land degradation. China suffers some of the most severe wind erosion in the world with 158.60×10^6 ha of total wind erosion area in 2018 with the most wind erosion occurring in arid and semiarid regions, such as deserts and sandy lands, where the local wind regime exhibits significant spatial differences (Chi, Zhao, Kuang, & He, 2019; Ministry of Water Resources of the People's Republic of China, 2018; Shen, Zhang, Wang, Zou, & Kang, 2018; Xu & Li, 2020).

Semi-buried sand barriers and plant cover practices are the most common practices used to reduce wind erosion within a natural sandy area, while gravel mulch is also commonly used in many construction project areas such as mining enterprises (Dai et al., 2019; Liu & Bo, 2020; Naghizade Asl, Asgari, Emami, & Jafari, 2019; Prosdocimi et al., 2016). These practices can effectively reduce wind erosion hazards. It has been demonstrated in the Taklimakan Desert that wheat straw used in checkerboard (straw-check) sand barriers may lower wind speeds by 33–90% and the sand transport rates by 60% (Cheng et al., 2015; Tian, Wu, Zhang, Lu, & Wang, 2015). The erosive resistance of gravel mulch is related to its coverage, pebble size, and spreading methods (Yuan, Lei, Mao, Liu, & Wu, 2009). They reported that roughness lengths increased with increased gravel coverage from 5 to 15%, but once the coverage exceeded 20%, the impacts on the roughness lengths were approximately equivalent to 0% coverage because the dense roughness elements resulted in an aerodynamically smoother surface (Dong, Wang, Liu, Li, & Zhao, 2002; Liu & Kimura, 2018). Plant cover practices have previously been considered as the ideal erosion reduction practice since the sand transport rates and the wind's flow patterns have been shown to be favourably impacted (Hong et al., 2020; Lv & Dong, 2012). Under specific wind speed conditions, the coverage and density of vegetation were negatively correlated with wind erosion such that when the vegetation coverage was less than 20%, there was substantially greater wind erosion (Li, Okin, Alvarez, & Epstein, 2007; Zhao, Zheng, & He, 2005; Dong, Fryrear, & Gao, 2000; Dong, Gao, & Fryrear, 2000). As an alternative method of wind erosion control, the rapid cultivation of biocrusts has been proven to be feasible and may be used as a practice for the short-term restoration of impaired ecosystems (Antoninka, Bowker, Reed, & Doherty, 2016; Bu et al., 2015; Bu, Wu, Yang, & Zheng, 2014; Doherty, Antoninka, Bowker, Ayuso, & Johnson, 2015; Maestre et al., 2016). Undisturbed biocrusts were shown to inhibit wind erosion at wind speeds of 25–30 m s^{-1} (Wang, Zhang, Zhang, & Han, 2004). Thus far, engineering and planting practices have primarily been used for wind erosion control, whereas the use of biocrust practices has been scientifically studied as a promising alternative practice for wind erosion reduction.

The use of combustible energy sources has increased the atmospheric concentrations of greenhouse gases and has caused increased global climate warming. For sustainable development in the future, using renewables such as wind energy, solar energy, and nuclear energy is the key to reducing the production of greenhouse gases in energy production (Solaun & Cerdá, 2019). In recent years, the development of solar photovoltaic power stations has rapidly increased in the NW of China. The cumulative installed photovoltaic power generation capacity of China reached 174 million kW by 2018, and within northwest China, the installed capacity of photovoltaic power stations has reached 50.03 million kW, which is the greatest photovoltaic power generation capacity of any Chinese region (National Energy Administration, 2018).

Large-scale disturbance and destruction associated with photovoltaic power station installation and operation have resulted in severe wind erosion hazards that pose a potential threat to the operation of the photovoltaic power stations and the already fragile sandy ecosystems. Unfortunately, there is not a mature system of wind erosion management practices currently available for these photovoltaic power station areas. Therefore, there is an urgent need to establish a comprehensive erosion-control management system and to study the efficiency and mechanisms of erosion control. Existing knowledge of the patterns and/or control of wind erosion under natural conditions has not proven to be applicable to these photovoltaic power stations located in sandy areas. Serious shortcomings in our knowledge and limited scientific studies, concerning the wind speed flow fields and wind erosion patterns surrounding the photovoltaic power stations, make it difficult to develop reasonable prevention measures to protect and sustain the fragile ecosystems. Etyemezian, Nikolich, and Gillies (2017) provided a first-order estimation of the mean wind flows resulting from a utility-scale solar photovoltaic facility that has been valuable for understanding these flows and for checking the representativeness of wind tunnel measurements with numerical modelling results.

To address the serious wind erosion hazards within the photovoltaic power station, different engineering treatments (wheat straw checkerboard, gravel mulch, red clay mulch, and combined practice), planting treatments (*Sedum aizoon* L. and *Pennisetum alopecuroides* [L.] Spreng), and biocrust treatments (cyanobacteria crust and moss-crust) were established within a typical photovoltaic power station in Mu Us Sandland of northwest China (Figure 1). The effectiveness of these practices in wind erosion reduction was evaluated to choose the type and placement of practices for optimal wind erosion reduction. We measured the observed wind speeds, sand transport rates, wind–sand flow structures, wind profiles, wind speed flow fields, and roughness at fixed locations. The primary objectives of this study were: (a) to

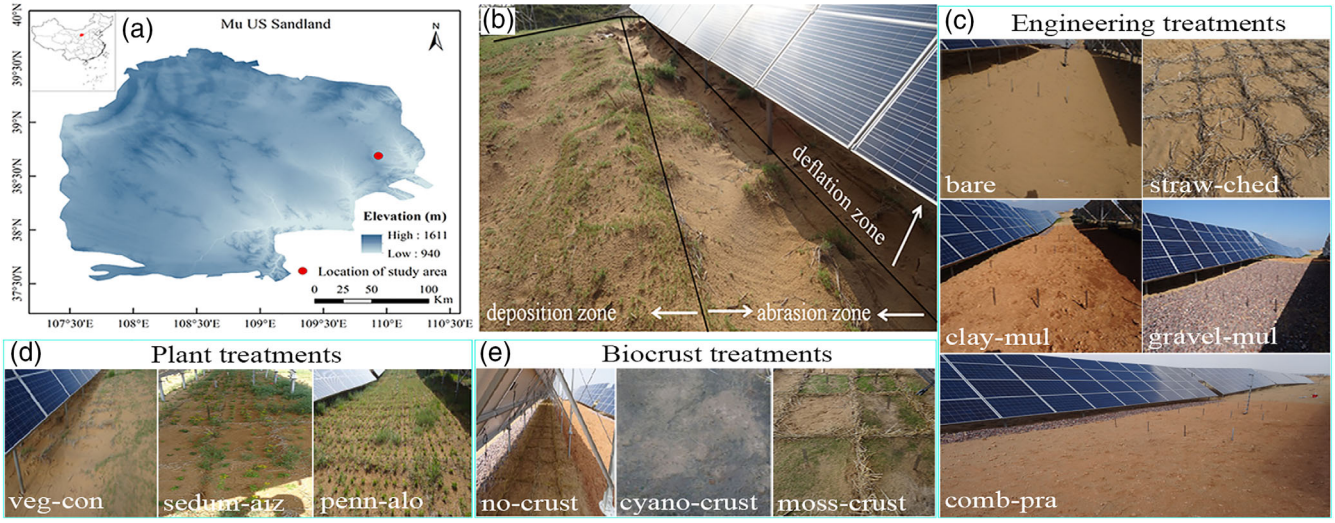

FIGURE 1 Location of the study area (a), locations of the deposition, abrasion, deflation zones (b), and the soil surface conditions of all treatments (c–e). Please note that the abbreviations refer to the treatments which are bare, bare land control; straw-check, wheat straw checkerboard; gravel-mul, gravel mulch; clay-mul, red clay mulch; comb-pra, gravel in the abrasion zone and red clay in the deposition zone; veg-con, control treatment in plant treatments that only placed with straw checkerboard; sedum-aiz, *Sedum aizoon* L. planting area; penn-alo, *Pennisetum alopecuroides* (L.) Spreng. planting area; no-crust, control treatment in biocrust treatments that only placed with straw checkerboard, cyano-crust, cyanobacterial crust mulch; moss-crust, moss crust mulch [Colour figure can be viewed at wileyonlinelibrary.com]

document the characteristics of the wind speed flow field within the photovoltaic power station; (b) to determine the efficiency and mechanism of engineering, plant, and biocrust treatments for erosion control; (c) to seek a protective management system for the reduction of wind erosion hazards within the photovoltaic power station projects that would also provide a practical reference for wind erosion control in similar projects.

2 | MATERIALS AND METHODS

2.1 | Study area

The study area is located on the southeastern edge of the Mu Us Sandland, near Dabaodang Town within southwestern Shenmu County of Shaanxi Province, China (38°41′31″N, 109°56′44″E) (Figure 1a). The average annual temperature is 8.9°C, and the annual average rainfall is 437.8 mm with large inter-annual variations. Southeasterly winds prevail during the summer (July–September), and northwesterly winds prevail during the remainder of the year. There are frequent sandstorms, and the average annual wind speed is 2.2 m s^{-1}, with a maximum of 3.0 m s^{-1} in April and a minimum of 1.7 m s^{-1} in September. The average seasonal wind speeds are 2.8 m s^{-1} in spring, 2.2 m s^{-1} in summer, 1.8 m s^{-1} in autumn, and 2.0 m s^{-1} in winter, and the daily average maximum wind speeds are 9.4 m s^{-1} in spring, 8.0 m s^{-1} in summer, 8.0 m s^{-1} in autumn, and 8.3 m s^{-1} in winter, respectively (Zhang et al., 2020). The primary vegetation includes *Artemisia ordosica* and *Salix cheilophila Schneid*, with sparsely distributed *Phyllostachys propinqua*, *Hedysarum scoparium*, *Hedysarum fruticosum*, and *Setaria viridis* (L.) *Beauv* (Yuan, Zhang, Bu, Yang, & Yuan, 2016). The soil at the study site was derived from aeolian sand and loess. This location is associated with a geomorphologic transition consisting of fixed to semifixed dunes and loess hills that typically have severe wind and water erosion (Jia, Yong, & Wang, 1993). There are also some limited agriculture, forestry, and animal husbandry activities practiced within this ecologically fragile zone. All the solar panels within the study area were simultaneously constructed by the same construction team using uniform specifications, size, and layout methods. To achieve the highest photovoltaic power generation, the solar panels are aligned north and south with the active solar receptive surface facing south. The characteristics of the sandy soil were homogeneous within the study area.

2.2 | Experimental layout

2.2.1 | Topographical description of the photovoltaic power station

Within the photovoltaic power station, the length and width of every solar panel's vertical projections were 18 and 3 m, respectively, and the distance between the solar panels to the next row was 7 m. Therefore, the area under one solar panel was 18 × 3 m, and the area between two adjacent solar panels was 18 × 7 m (Figure 2a). The wind erosion conditions under the solar panels and between the rows of solar panels were significantly different.

Slight wind erosion on the surface layer occurred under the solar panels, which were defined as deflation zones with a typical size of 18 × 3 m. Both erosion and deposition occurred between the rows of solar panels. Within this area, a distinct V-shaped trench (typically

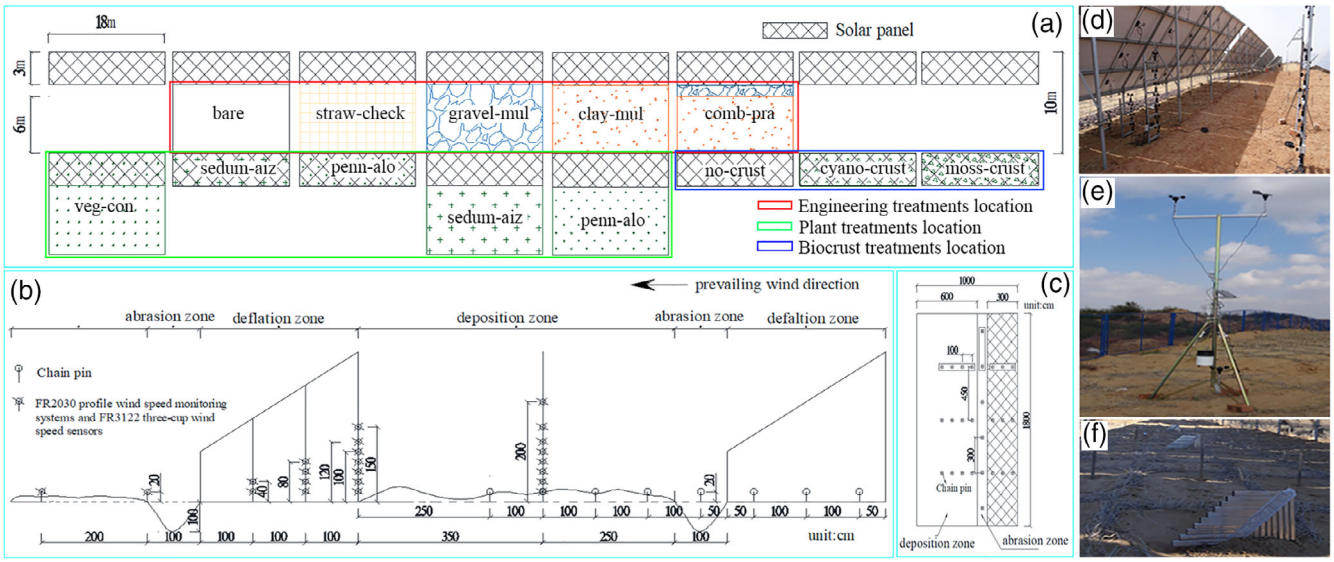

FIGURE 2 Relative position schematic of each treatment (a) and a side view of the instrumentation placement d photographs. The layout position and height of chain-pins, FR2030 profile wind speed monitoring systems and FR3122 three-cup wind speed sensors (b); the chain-pins layout position in deflation zones and between the solar panels (c); FR2030 profile wind speed monitoring systems and FR3122 three-cup wind speed sensors (d); HOBO U30 meteorological station; *F* showed the 10-step sand samplers (e) [Colour figure can be viewed at wileyonlinelibrary.com]

1-m width and 1-m depth) was formed within 1 m of the wind outlet of the solar panel. The remaining area (between the outer edge of the V-shaped trench and the deflation zone under the next row of solar panels) formed approximately a 40 cm depth of deposition. We defined these two areas as an abrasion zone and deposition zone with dimensions that were 18 × 1 m and 18 × 6 m, respectively (Figure 1b). This phenomenon of the trench formation and deposition zones uniformly occurred within the study area. Therefore, the zones of our experimental design are between the rows of solar panels (including the abrasion zone and deposition zone) and the deflation zones beneath the solar panel rows. In August 2014, prior to the beginning of the study, the entire study area was leveled and restored to the original landforms that coincided with the completion of construction for the photovoltaic power station.

2.2.2 | Treatments layout

The study included engineering, plant, and biocrust treatments with the placement and the relationship of the treatments as shown in Figure 2a and described in Table 1. The five engineering treatments included bare land controls (bare), wheat straw checkerboard (straw-check), gravel mulch (gravel-mul), red clay mulch (clay-mul), and combined practices (comb-pra), which were placed within the region between the rows of solar panels. The bare, straw-check, gravel-mul, and clay-mul treatments were single practice treatments, while the comb-pra treatment was a combined practice treatment that consisted of gravel placed on the soil surface within the abrasion zone and red clay placed on the soil surface within the deposition zones, respectively. The materials used in the study were obtained from resources within the surrounding area. Gravel and red clay were placed artificially with a shovel after having been transported to the study area.

S. aizoon L. (sedum-aiz), and *P. alopecuroides* (*L.*) Spreng. (penn-alo) were plant treatments, which were placed within the deflation zone and between the rows of solar panels, respectively. The low survival rate of *S. aizoon* L. seed and high survival rate of *P. alopecuroides* (L.) Spreng. seed caused different planting methods. Transplantation is suitable for *S. aizoon* L. and broadcasting for *P. alopecuroides* (L.) Spreng, respectively. Wheat straw checkerboards were placed within the treatment area to provide initial protection for plant growth at the beginning of the study. Therefore, there was one deflation zone and an entire region between the rows of solar panels where straw checkerboard was placed as the control of the plant treatments (veg-con). Wheat straw was placed on the surface after planting to prevent the seeds from being blown away, reduce water evaporation, and improve survival rates. Water was applied once every two days for 1 month at which time the wheat straw was removed and no additional water was applied.

Cyanobacterial crust mulch (cyano-crust) and moss-crust mulch (moss-crust) were the biocrust treatments that were placed on the soil surface within the deflation zones. Wheat straw checkerboards were initially placed within the zones to protect the growth and development of the biocrust at the beginning of the study. Therefore, the placement of a straw checkerboard within the deflation zones served as the control of the biocrust treatments (i.e., no crust was placed on the controls). Inoculum with a 10-mm thickness for the moss-crust and cyano-crust was collected from the surrounding area and from Yangguanhaize Village, which is a Yulin City approximately 100 km away from the study area, respectively. After collection, the sampled inoculum was dried in the shade under natural conditions and made uniform using a plant sample pulverizer. Afterward, the pulverized

TABLE 1 Names, abbreviations, layout area, and descriptions of the different treatments and identification of its usage as an engineering, plant, or biocrust type of erosion-control practice

Treatments		Abbreviation	Layout location and descriptions	
			Between the rows of the solar panel area (including abrasion and deposition zones)	Deflation zones
Engineering treatment	Bare land control	bare	The original bare sandy land was maintained.	×
	Wheat straw checkerboard	straw-check	The size of the wheat straw checkerboard is 1 m × 1 m.	×
	Gravel mulch	gravel-mul	A layer of gravel 3–7 cm in diameter was placed on the surface.	×
	Red clay mulch	clay-mul	A layer of red clay 10 cm thick was placed on the surface.	×
	Combined measures	comb-pra	Gravel and red clay were placed in the abrasion and deposition areas, respectively.	×
Plant treatment	Vegetation control	veg-con	Only wheat straw checkerboard was placed as the control treatment.	
	Sedum aizoon L.	sedum-aiz	Transplantation, 15 plants m^{-2}, the straw checkerboard was placed to provide stable colonization conditions before plantation.	
	Pennisetum alopecuroides (L.) Spreng.	penn-alo	Broadcasting, 15 kg ha^{-1}, the straw checkerboard was placed to provide stable colonization conditions before plantation.	
Biocrust treatment	Biocrust control	no-crust	×	Only straw checkerboard was placed as the control treatment.
	Cyanobacterial crust mulch	cyano-crust	×	Straw checkerboard was placed to provide stable colonization conditions. *Microcoleus vaginatus*, *Tolypothrix tenuis*, and *Phormidium* were dominant species.
	Moss-crust mulch	moss-crust	×	Straw checkerboard was placed to provide stable colonization conditions. *Bryum argenteum* is dominant species.

Notes: × represents the treatment did not layout in this subdivision. The size of the straw checkerboard in the plant and biocrust treatments is 1 m × 1 m. In the deflation zones, the measurement indicators included sand transport rates and sand erosion–deposit budges. These two indicators for each treatment within this area had three repetitions. Between the rows of the solar panels, the measurement indicators included wind speed profiles, sand transport rates, and sand erosion–deposit budgets. The measuring indicators for characterizing the wind speed profiles and the sand transport rates were placed within the deposition zone; their measurement results were used to determine the wind speed profiles and the sand transport rates of the areas between the rows of solar panels (including the abrasion zone and deposition zone). Each treatment between the rows of the solar panels had 10 and 3 repetitions for the wind speed profiles and the sand transport rates, respectively. The chain-pins, which are used to measure the sand erosion–deposit budgets, were placed both in the abrasion and deposition zones with three repetitions for each treatment within the abrasion zone and deposition zone.

samples were spread evenly within the appropriate plot areas at a rate of 500 g m^{-2}. A BG11 nutrient solution and Hoagland nutrient solution were applied to the cyanobacterial crust and moss-crust at a rate of 3 L m^{-2} every 2 days, respectively. The cultivation period for the biocrust treatments was 75 days.

2.3 | Measurement indicators and methods

2.3.1 | Measurement indicators

We used efficiency and mechanism indicators to evaluate treatment effects. Efficiency indicators represent the wind erosion reduction efficiencies of the various treatments on the sand transport rates, wind–sand flow structure, and sand erosion–deposit budgets. The sand transport rates refer to the quantities of sediment transported by the wind per unit of surface area and time. The distribution of sediment within the sand flow along the height of the flow is called the wind–sand flow structure (Butterfield, 1991). The sand erosion–deposit budgets refer to the difference between the accumulated amounts and the surface material transported by the wind at a certain time. Mechanism indicators can be used to explain the reasons for wind erosion reduction of different treatments, including the wind speed flow field, wind speed profiles, and the aerodynamic roughness ($z0$). The wind speed flow field refers to the distribution of the wind speed over space, and the wind speed profile refers to the distribution of the wind speed along with the height above the soil surface (Bagnold, 1942). Aerodynamic roughness ($z0$) is an index of the effects

of the ground surface on the airflow and usually represents a geometric height of zero wind speed that is calculated using the wind speeds at different heights (Borak, Jasinski, & Crago, 2005; Liu & Dong, 2003).

For plant treatments and biocrust treatments within the deflation zones, the measurement indicators included sand transport rates and sand erosion–deposit budgets. These two indicators for each treatment within this measurement area had three repetitions. For engineering and plant treatments between rows of the solar panels, the measurement indicators included wind speed profiles, sand transport rates, and sand erosion–deposit budgets. The measuring indicators for characterizing the wind speed profiles and the sand transport rates were placed within the deposition zone. The measurement results were used to determine the wind speed profiles and the sand transport rates of the areas between the rows of solar panels (including the abrasion zone and deposition zone). These two indicators for each treatment between the rows of the solar panels had 10 and 3 repetitions for the wind speed profiles and the sand transport rates, respectively. The chain-pins, which were used to measure the sand erosion–deposit budgets, were placed both in the abrasion and deposition zones with three repetitions for each treatment within the abrasion zone and deposition zone.

2.3.2 | Measurement methods

The influence of the solar panels on the wind speeds was synchronously measured at 20 and 200 cm heights from April 23 to 26, 2015, within the peripheral area outside of the placement of the solar panels and within the bare land control treatment between the rows of the solar panels. Within the peripheral area, the wind speeds were measured using a HOBO U30 meteorological station (Figure 2e) (Onset Computer Corporation, Inc.), which collected data measurements in 1 s intervals with the 10 min averages also being automatically recorded. Between the rows of the solar panels, an FR2030 profile wind speed monitoring system combined with an FR3122 three-cup wind speed sensor was used (Figure 2d) (Onset Computer Corporation, Inc.), which collected data measurements in 1 s intervals with the 1 min averages also being automatically recorded. During the study, we obtained a total of 401 and 3,903 wind datasets within the peripheral areas outside the placement of the solar panels and within the bare land control treatment between the rows of the solar panels, respectively.

The wind speed flow field within the bare land control treatment between the rows of the solar panels was measured to determine the vertical variations of subsurface wind speeds under the influence of the solar panels using FR2030 profile wind speed monitoring systems combined with FR3122 three-cup wind speed sensors. Six groups of FR3122 three-cup wind speed sensors were used to simultaneously measure the wind speeds at different heights around the solar panels (Figure 2b). The highest measured height increased gradually from the wind outlet to the wind inlet. Measurements were taken 3 m from the front of the wind outlet where wind speeds at a 20 cm height were measured. As a point of reference, we took this position as the origin point (0,0) for the direction of the wind outlet to the wind inlet as a positive direction in 1-m intervals to describe the position of the other instruments in a detailed layout as follows: (a) at position (2,0), the sampling location was the same as the origin point, with wind speeds measured at a 20-cm height; (b) at (4,0), 1 m behind the wind outlet, the wind speeds were measured at heights of 20 and 40 cm; (c) at (5,0), 2 m behind the wind outlet, the wind speeds were measured at heights of 20, 40, 60, and 80 cm; (d) at (6,0), the wind speeds were measured at heights of 20, 40, 60, 80, 100, 120, and 150 cm; and (e) at (9.5,0), 3.5 m behind the wind inlet, the wind speeds were measured at heights of 20, 40, 60, 80, 100, 120, 150, and 200 cm. There were a total of 23 FR3122 three-cup wind speed sensors used to make simultaneous measurements from April 23, 2015 to April 26, 2015. Wind speed measurements were also automatically recorded on a 1-min basis and these measurements were used to graphically display the wind speed flow fields.

The FR2030 profile wind speed monitoring systems combined with the FR3122 three-cup wind speed sensors were set in every treatment between the rows of the solar panels to simultaneously measure wind speeds at heights of 20, 40, 60, 80, 100, 120, 150, and 200 cm (Figure 2b). Measurements in 1 s intervals and 1 min averages were automatically recorded, and then the recorded data measurements were used to determine the wind speed profiles to calculate $z0$. We assumed that in neutral or near-neutral layers, the wind speed within the surface layer presents a logarithmic relationship within the height distribution. Using the average wind speeds as a basis to calculate $z0$ has been shown to improve the reasonableness and accuracy of results (Yang, 1996). Therefore, the wind speed profile and calculation of $z0$ were based on an average of 10 groups of data measured at 10-min intervals. The computation of $z0$ was calculated from the average wind speed profiles using the following equations (Dong et al., 2000; Liu & Dong, 2003; Zhang et al., 2016):

$$u = a + b \ln z, \tag{1}$$

$$z0 = e^{(-a/b)}, \tag{2}$$

Where: u is the wind speed (m s^{-1}) at height z; a and b are the intercept and slope of the logarithmic function of the wind speed profiles, respectively, and determined by means of least-squares curve fitting.

Sand transport rates were measured using three 10-step sand samplers that were placed along the axis within each experimental area with the sand inlet of each sampler parallel to the wind direction (Figure 2f). The sand sampler was a passive sampler and similar to the WITSEG sampler designed by Cold and Arid Regions Environmental and Engineering Research Institute, Chinese Academy of Sciences (Dong, Sun, & Zhao, 2004). The height of the sand samplers was 25 cm and sectioned into 10 blown sand inlets such that every inlet was 2.5×2.5 cm and connected with a sand chamber. Every sand sampler was positioned within the experimental area such that each sampler and the series of measurements made by each sampler served as a repetition. To reduce the variability caused by the external

environment, the sand mass of every sand sampler was randomly measured three times (as a repeated measure) and averaged to analyze the differences among different treatments. Each measurement period was 24 hr and the mass of sand within each chamber was measured using an electronic scale with an accuracy of ten-thousandths of a gram. The sand transport rate was obtained using the following Equation (3) (Ma et al., 2010).

$$Q = W/(a \cdot T), \quad (3)$$

Where: Q is the sand transport rate, g ($cm^{-2}hr$); W is the sand mass in the sand sampler, g; a is the area of the sand sampler, 6.25 cm^2; and T is the observation time, hr.

Chain-pins, 60 cm in length, were used to measure the sand erosion–deposit budget and were arranged uniformly after the application of all treatments to ensure the consistency of the initial measured height and measured time. Between the solar panels, the chain-pins were placed in three rows and three columns within the deposition zone and 30 cm vertically into the ground, with six chain-pins that were equally divided for placement within the abrasion zone and 20 cm vertically into the ground (Figure 2c). In deflation zones, the chain-pins were placed in three rows and three columns, and 20 cm vertically into the ground. The mean of the chain-pins' value within each column in the deflation zones or deposition zones was regarded as a repetition, and the mean of every two chain-pins' value in the abrasion zones was regarded as a repetition. Therefore, there were three repetitions of every treatment in each zone. The observed period of wind erosion was from October 15, 2014, to October 15, 2015. We measured the vertical length (H) of the chain-pins on the ground to calculate the sand erosion–deposit budget by 'H'. Fine particles and associated nutrients in the soil that have been depleted directly by wind erosion have been shown to be primary contributors to soil degradation (Yan et al., 2013). Therefore, we suppose that the hazards caused by erosion have more serious impacts than deposition. In this study, practices that caused deposition were found to be more effective in reducing wind erosion, with smaller values of deposition, and displayed improved results in the reduction of erosion within the corresponding treatments.

2.4 | Data analysis

To explore possible differences in the sand transport rate, erosion, and deposition among different treatments, and at different heights above the ground, we used a permutated multivariate analysis of variance (PERMANOVA) procedure with the Primer-PERMANOVA+ package (Anderson, Gorley, & Clarke, 2008). The PERMANOVA is a nonparametric multivariate statistical test and procedure that permutes a distribution based on a Euclidean distance matrix, and calculates a permutated F-statistic and associated p value, similar to a one-way ANOVA, but without any assumptions of normality. The PERMANOVA procedure then allowed us to conduct a number of multiple comparisons to test the differences among different treatments using the t-distribution. Analyses were conducted separately for the engineering, plant, and biocrust treatments with separate analyses in the deflation zones and between the rows of the solar panels. It is understood that our three measurements of sand transport rates and the sand erosion–deposit budgets are pseudo-replicates in the sense that the measurements were placed under the same photovoltaic solar power station. Nevertheless, the measurements provided us with reasonable indications of potential differences among the various treatments because of the relatively large size of the study area, which should also partially minimize the impacts of the random errors. Wind speed data were processed using Microsoft EXCEL 2016 and analyzed using a one-way ANOVA with SPSS 19.0 statistical software (SPSS Inc., Chicago, IL, USA). Means comparisons were performed following significant differences in the mean effects using a protected Tukey's Honest Significant Difference ($p \leq 0.05$). The wind speed profile equation was simulated using Microsoft EXCEL 2016 and the figures were drawn using SURFER 14.0 (Golden Software, USA) and ORIGIN 2017 (OriginLab, USA).

3 | RESULTS

3.1 | Characteristics of the wind speed and the wind speed flow field between solar panels

The average wind speeds at the heights of 20- and 200-cm within the peripheral area were 1.51 and 3.64 m s^{-1}, respectively, while between the rows of solar panels the average wind speeds were 1.06 and 1.40 m s^{-1}, respectively. Wind speeds between the rows of solar panels were reduced by 29.8 and 61.5% at the heights of 20 and 200 cm when compared with the wind speeds within the peripheral area. Therefore, the arrangement of the solar panels significantly decreased wind speeds. Figure 3 displays the wind speed distribution around the solar panel, and we can see that the wind speed at location A (air outlet) was higher than location B (air inlet).

3.2 | Effects of various treatments on sand transport rates

Among the engineering treatments, the total horizontal sand transport rates of the control treatment was 2,801.8 g ($cm^{-2} \cdot hr) \cdot 10^{-4}$, and formed the relative basis of comparison for the other treatments in wind erosion reduction. The treatments displayed a rank order trend from highest to lowest reductions in wind erosion as comb-pra (87%) > gravel-mul (78%) > clay-mul (74%) > straw-check (51%). The results of the PERMANOVA analyses determined there were significant differences among all treatments ($F = 99.81$, $p < 0.01$). Multiple means comparisons generally indicated that there were significant differences among the bare land control and the straw-check treatment and the other treatments although oftentimes there were no significant differences between the gravel-mul and comb-pra treatments (Table 2). The results of multiple comparisons of the sand transport

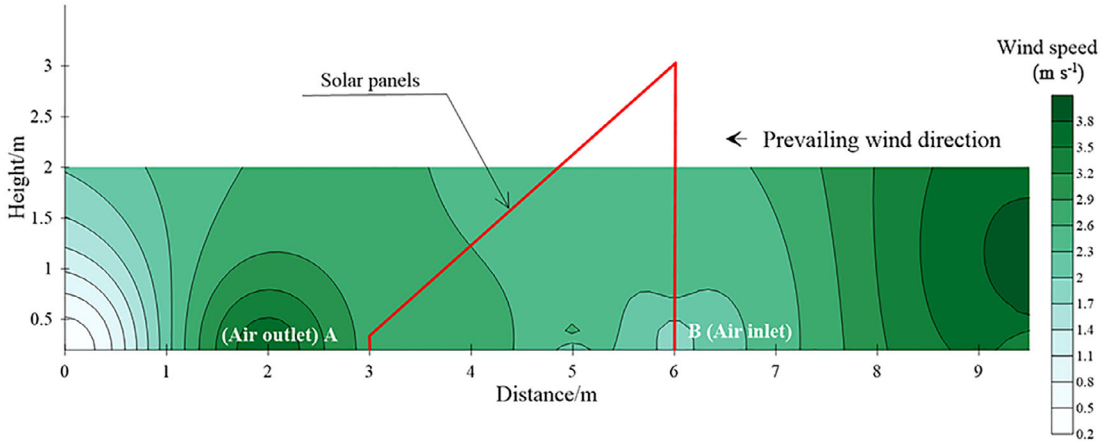

FIGURE 3 Diagram of the wind speed flow field in regards to the side view of a solar panel placement where the wind speed flow lines are shown for the inlet and outlet areas of the solar panel and are shown for approximately a 9-m distance and a 2-m height above the soil surface [Colour figure can be viewed at wileyonlinelibrary.com]

rates at different heights showed within the 0–10 cm intervals that the differences among all treatments were significant. Within the 10–25 cm intervals, there were no significant differences between the control and the straw-check treatments although these two treatments differed from the gravel-mul, clay-mul, and comb-pra treatments, which generally displayed no differences among themselves (Table 2).

Whether between the rows of solar panels or in the deflation zones, the sand transport rates significantly decreased within the total horizon distance for the sedum-aiz and penn-alo treatments (with F values between 146.42 and 12.75, ($p < 0.01$), and with F values less than 12.752, ($p < 0.05$), respectively). In the deflation zones, the total horizontal sand transport rates of sedum-aiz and penn-alo treatments were 383.2 and 309.6 g (cm^{-2}·hr)·10^{-4}, respectively, which produced 20% and 36% reductions compared with the control (480.1 g (cm^{-2}·hr)·10^{-4}), respectively. There were no significant differences between the sedum-aiz and penn-alo treatments. Between the rows of solar panels, the total horizontal sand transport rate of the veg-con treatment displayed a maximum value of 2,969.7 g (cm^{-2}·hr)·10^{-4}, while the sedum-aiz and penn-alo treatments produced reductions in the total horizontal sand transport rate of 86 and 78%, respectively, in comparison with the control. Mean comparisons indicated that the veg-con treatment significantly differed in comparison to the other treatments while there were no differences in the total horizontal sand transport rates displayed between the sedum-aiz and penn-alo treatments except for the 17.5–20 cm heights (Table 2).

Biocrust treatments also displayed statistically significant reductions on the total sand transport rates within the deflation zones ($F = 104.98$, $p < 0.05$). The total horizontal sand transport rates of the cyano-crust and moss-crust treatments were 359.1 and 297.5 g (cm^{-2}·hr)·10^{-4}, respectively, which represented reductions of 65 and 71%, respectively, compared with the control (1,033.4 g (cm^{-2}·hr)·10^{-4}). No significant differences in the sand transport rates were displayed between the cyano-crust and moss-crust treatments (Table 2).

3.3 | Effects of various treatments on wind–sand flow structure

The relative sand transport rate index is used to describe the wind–sand flow structure that utilizes the percentages of transferred sand quantities within each height interval of the total distribution.

As shown in Figure 4, the sand transport rates associated with all the treatments gradually decreased with increased height and are consistent with Butterfield's findings that displayed a similar pattern of reductions (Butterfield, 1991). The sand transport rates observed for the straw-check, gravel-mul, and clay-mul treatments decreased rapidly below the 12.5 cm height, whereas the rate of decrease was relatively unchanged above the 12.5 cm height (Figure 4a).

Within the 0–10 cm height range, the sand transport rates observed for the plant treatments within the deflation zones decreased rapidly, whereas the rate of decrease was relatively unchanged within the 10–25 cm height range (Figure 4b). Between the rows of the solar panels, the sand transport rates observed for the sedum-aiz treatment were drastically reduced within the 0–15 cm height range, whereas the rates observed for the penn-alo treatment showed stable changes within the 0–25 cm height range (Figure 4c).

The sand transport rates of the cyano-crust and moss-crust treatments displayed a relatively homogenous distribution above the treatments, and the relative sand transport rate of each layer stayed within a range of 8–12%. The sand transport rates of the no-crust treatment drastically decreased within the height range of 0–10 cm, whereas the decrease was relatively constant within the height range of 10–25 cm (Figure 4d).

3.4 | Effects of various treatments on sand erosion and deposition

Within the abrasion zones, the different engineering and plant treatments displayed significant differences on the sand erosion–deposit

TABLE 2 Locations and sand transport rates for the engineering, plant, and biocrust treatments at various height intervals above the ground surface in the solar panel area of the photovoltaic power station

Practice treatment		Location	Height above the ground surface (cm)										
			0–2.5	2.5–5.0	5.0–7.5	7.5–10	10–12.5	12.5–15	15–17.5	17.5–20	20–22.5	22.5–25	Total
Engineering treatment	Bare land control	Between the rows of the solar panels	1,027.5a	603.0a	370.2a	219.9a	144.4a	108.8a	91.1a	81.2a	77.3a	78.2a	2,801.8a
	Wheat straw checkerboard		353.9b	272.9b	186.4b	137.3b	99.3a	79.5a	68.7a	59.0b	52.5b	70.9a	1,380.4b
	Gravel mulch		176.5c	111.1c	69.1d	51.6d	40.2b	34.3b	32.2b	30.8b	30.0c	29.3b	605.1 cd
	Red clay mulch		201.8c	131.2bc	92.5b	76.1c	54.8b	46.7b	38.3b	35.2b	31.3c	29.3b	737.1c
	Combined measures		60.0d	49.4d	42.0 cd	35.3d	31.1b	30.4b	34.9b	27.3b	31.7c	33.5b	375.5d
Plant treatment	Vegetation control	Deflation zone	111.9b	56.4a	44.7a	34.6a	36.7a	42.2a	40.7a	41.8a	39.4a	31.9a	480.1a
	Sedum aizoon L.		188.2a	41.2a	33.0a	26.7a	22.5ab	19.1b	14.3b	15.8b	12.0b	10.5b	383.2ab
	Pennisetum alopecuroides (L.) Spreng.		97.6b	67.2a	53.6a	27.5a	18.0b	10.6b	7.4b	13.6b	7.7b	6.3b	309.6b
	Vegetation control	Between the rows of the solar panels	1,066.1a	576.8a	361.9a	304.5a	216.9a	143.8a	92.2a	80.2a	65.6a	61.8a	2,969.7a
	Sedum aizoon L.		173.5b	60.9b	42.8b	38.6b	36.0b	19.4b	14.6b	11.9c	7.3b	6.4b	411.4c
	Pennisetum alopecuroides (L.) Spreng.		190.5b	140.9b	121.3b	49.7b	46.1b	30.2b	20.1b	37.8b	12.4b	10.9b	659.9b
Biocrust treatment	Biocrust control	Deflation zone	350.6a	269.4a	103.8a	72.3a	57.6a	32.5a	33.2a	36.1a	34.3a	43.8a	1,033.5a
	Cyanobacterial crust mulch		43.5b	41.2b	39.2b	36.8b	35.9b	32.9a	31.2a	30.6a	30.8a	37.0a	359.1b
	Moss-crust mulch		31.4b	29.6b	29.8b	29.4b	28.3b	28.2a	29.2a	28.8a	28.4a	34.7a	297.5b

Notes: Please note that all sand transport values are given in units of [g (cm^{-2}·hr)·10^{-4}]. Different letters indicate significant differences at the $p \leq .05$ level within each column using permutated multivariate analysis of variance (PERMANOVA) for means comparisons.

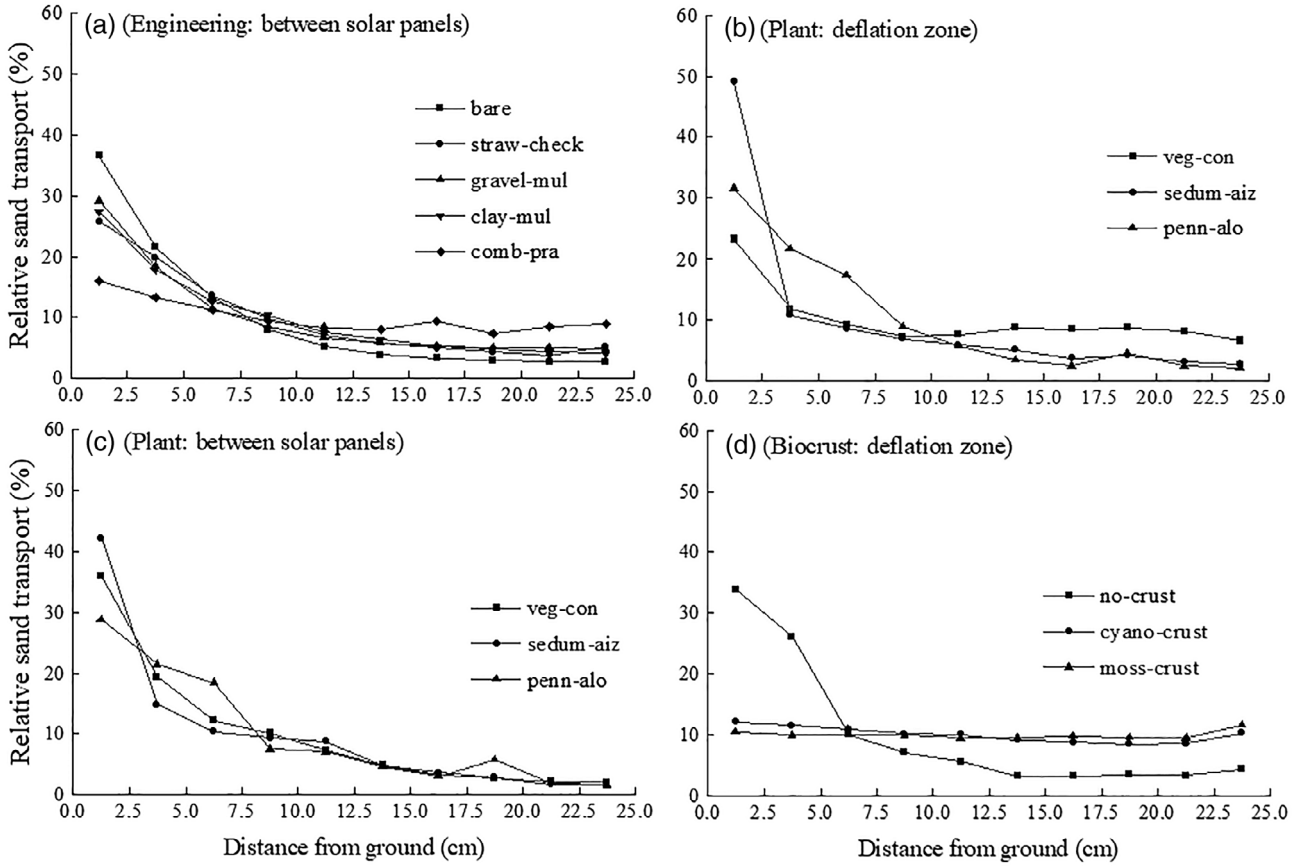

FIGURE 4 The relative sand transport rates versus distance above the soil surface for the engineering, plant, and biocrust treatments where the treatments are bare, bare land control; straw-check, wheat straw checkerboard; gravel-mul, gravel mulch; clay-mul, red clay mulch; comb-pra, gravel in abrasion zone and red clay in the deposition zone; veg-con, control treatment in plant treatments that only placed with straw checkerboard; sedum-aiz, *Sedum aizoon* L. planting area; penn-alo, *Pennisetum alopecuroides* (L.) Spreng. planting area; no-crust, control treatment in biocrust treatments that only placed with straw checkerboard, cyano-crust, cyanobacterial crust mulch; moss-crust, moss crust mulch

budget (engineering: F = 1,046.6, $p < 0.001$; plant: F = 211.094, $p < 0.01$). The control treatment produced 23.8 cm of erosion losses while the straw-check treatment only produced 6.0 cm of erosion losses, which was a 75% reduction in erosion losses compared with the control. The gravel-mul, clay-mul, and comb-pra treatments resulted in depositions of 1.0, 1.6, and 3.1 cm, respectively, and the sand erosion–deposit budgets decreased by 104, 107, and 113%, respectively, in comparison to the control. Multiple means comparisons indicated there were significant differences among the different engineering treatments although no distinct patterns were observed (Figure 5a). Sedum-aiz and penn-alo treatments resulted in 3.2 and 3.8 cm of erosion losses, which decreased the budget by 65 and 58% compared with the control (9.2 cm of erosion losses), respectively. Further analysis showed there were significant differences between the veg-con and the sedum-aiz and penn-alo treatments, but no significant differences existed between the sedum-aiz and penn-alo treatments (Figure 5b).

Within the deposition zones associated with the engineering treatments, the control and straw-check treatments resulted in erosion losses, which were 1.6 and 4.2 cm, respectively, while the remaining treatments produced lower quantities of deposition. The clay-mul and comb-pra treatments both resulted in depositions of 1.4 cm that performed better when compared with the other engineering treatments (Figure 5a). The results for the plant treatments within the deposition zones showed the veg-con control treatment resulted in 1.0 cm of gravel deposition, while the sedum-aiz and penn-alo treatments resulted in 0.6 and 0.5 cm of gravel erosion, respectively. There were no significant differences between the sedum-aiz and penn-alo treatments, but both treatments were significant in comparison with the veg-con control treatment (Figure 5b).

Within the deflation zones, the plant treatments produced different patterns of erosion losses. The veg-con, sedum-aiz, and penn-alo treatments resulted in 2.3, 1.4, and 1.8 cm of soil erosion, respectively. The sedum-aiz and penn-alo treatments reduced the quantities of erosion by 40 and 22% compared to the control, respectively, but there were no significant differences between the sedum-aiz and penn-alo treatments (Figure 5b). The cyano-crust and moss-crust biocrust treatments had depositions of 0.3 and 0.5 cm, respectively, while the control exhibited 3.5 cm of soil erosion. Compared with the control, the sand erosion–deposit budget associated with the cyano-

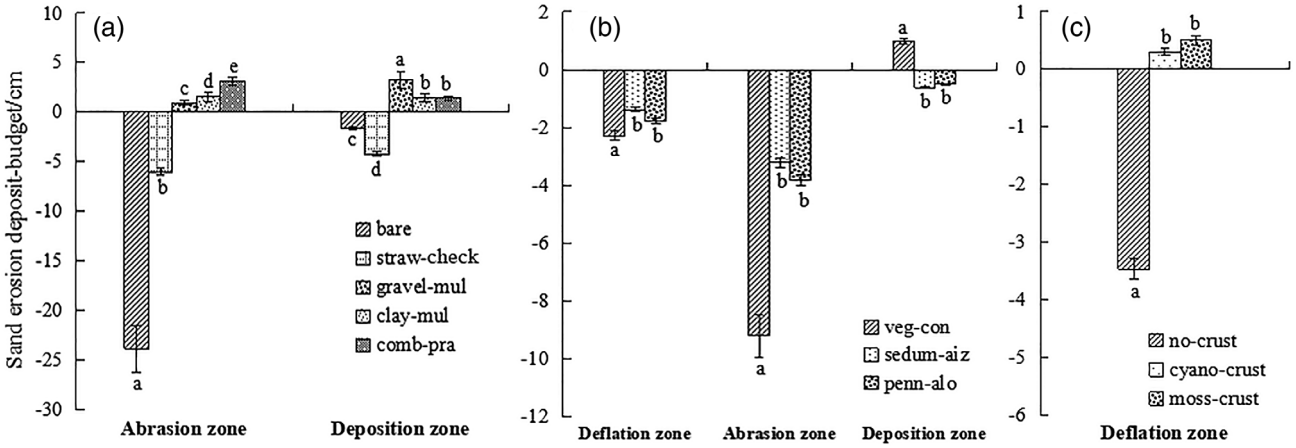

FIGURE 5 The sand erosion-deposit budget associated with the engineering, plant, and biocrust treatments where the treatments are bare, bare land control; straw-check, wheat straw checkerboard; gravel-mul, gravel mulch; clay-mul, red clay mulch; comb-pra, gravel in abrasion zone and red clay in the deposition zone; veg-con, control treatment in plant treatments that only placed with straw checkerboard; sedum-aiz, *Sedum aizoon* L. planting area; penn-alo, *Pennisetum alopecuroides* (L.) Spreng. planting area; no-crust, control treatment in biocrust treatments that only placed with straw checkerboard, cyano-crust, cyanobacterial crust mulch; moss-crust, moss crust mulch

crust and moss-crust treatments decreased by 109 and 114%, respectively, although there were no significant differences between the cyano-crust and moss-crust treatments (Figure 5c).

3.5 | Effects of various treatments on the wind speed profile

The wind speeds observed above the engineering and plant treatments generally increased with height (Figures 6 and 7), which was expected and conforms to the logarithmic distribution law (Wu, Zhang, Tian, Zhao, & Jia, 2013; Zhang, Li, et al., 2016). The range of wind speeds observed above the bare check treatment and the gravel-mul treatment were relatively dispersed while the wind speeds above the other engineering treatments were relatively concentrated and displayed somewhat regular distribution patterns. The average wind speed distribution with height indicated that compared with the control, the other engineering treatments effectively reduced the wind speeds (Figure 6f). At the height of 20 cm, the average wind speed observed above the control treatment was 4.7 m s^{-1}, while straw-check, gravel-mul, clay-mul, and comb-pra were 2.4, 4.6, 2.6, and 2.8 m s^{-1}, respectively, which represent reductions of 49, 2, 45, and 40% compared with the control, respectively. The largest reductions of the wind speed were observed at a height of 20 cm for the straw-check treatment, while the clay-mul treatment displayed the largest reductions at the other heights of measurement. There were significant differences among the bare treatment when compared with the straw-check and gravel-mul treatments at every height, while the differences in means comparisons between the clay-mul and comb-pra treatments were not significant (Table S1).

For the plant treatments, the range of wind speeds was relatively concentrated above the control treatment and was relatively dispersed above the sedum-aiz treatment (Figure 7). Above the sedum-aiz treatment, the wind speed increased rapidly within the height range of 20–40 cm and then increased slowly within the height range of 40–200 cm. Above the penn-alo treatment, the wind speed gradually increased throughout the entire height range, but the changes between the adjacent height intervals were apparently random. At the height of 20 cm, both the sedum-aiz and penn-alo treatments slightly reduced the average wind speeds compared with the control (2.38 m s^{-1}), but the means comparisons indicated there were no significant differences among the plant treatments. The penn-alo treatment increased the average wind speeds above 20 cm, however, the results of the one-way ANOVA analysis showed that plant treatments had no significant effects on wind speeds at different height intervals except for the 40–60 cm height intervals where statistically significant differences were observed (Table S1). The wind speeds associated with the biocrust treatments gradually increased with the height above the soil surface and were similar to the results observed for the engineering treatments.

3.6 | Aerodynamic roughness (z0)

Table 3 shows the results of a logarithmic function applied to the wind profiles and the resulting z0 calculations. The fitting coefficients all exceeded 0.8 and indicated the fitting results were reliable.

The roughness under the engineering treatments followed the trend of straw-check (0.748 cm) > clay-mul (0.163 cm) > bare = comb-pra (0.078 cm) > gravel-mul (0.003 cm). Compared to the control, the roughness may be divided into three categories: increased, decreased, and neutral. The roughness of the straw-check and clay-mul treatments was 9.6-times and 2.1-times greater than the bare land, respectively. The roughness under the gravel-mul treatment was reduced by an order of magnitude in comparison to the control and may be considered as approximately 0 cm.

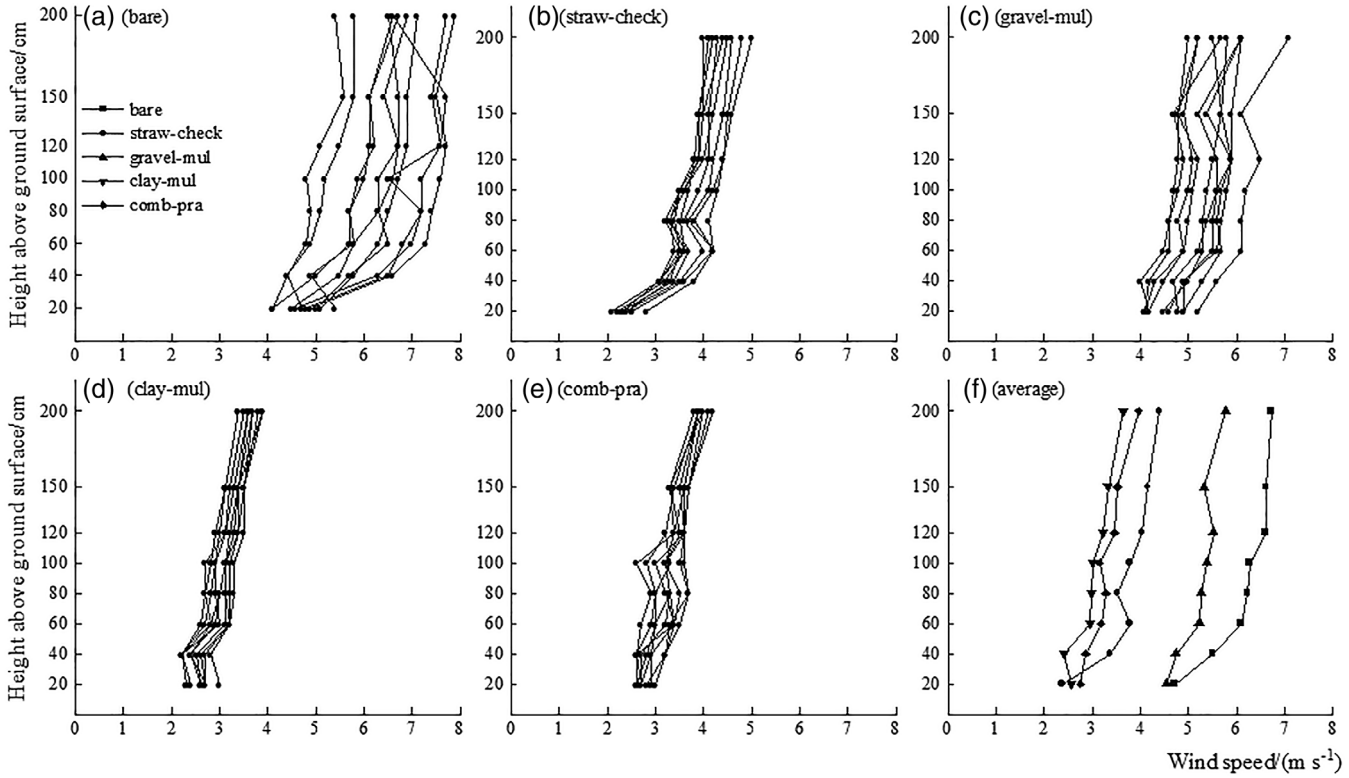

FIGURE 6 The changes in wind speed with height above the soil surface for the engineering treatments where the treatments are bare, bare land control; straw-ched, wheat straw checkerboard; gravel-mul, gravel mulch; clay-mul, red clay mulch; comb-pra, gravel in abrasion zone and red clay in the deposition zone

The sedum-aiz and penn-alo treatments both increased the roughness and followed the trend of penn-alo (0.413 cm) > sedum-aiz (0.338 cm) > veg-con (0.317 cm). Compared with the control, the sedum-aiz treatment increased the roughness by 6.6% while the penn-alo treatment increased the roughness by 30.3%. The erosion-control mechanism of biocrusts is generally similar to the behavior displayed by gravel mulch such that the aerodynamic roughness was increased and the near-surface wind speed flow field was altered.

4 | DISCUSSION

4.1 | The construction of the photovoltaic power station aggravated the wind erosion hazard

It has been shown that the presence of obstacles has the potential to change the surrounding wind flow field distribution and wind speed, and thus have significant effects on erosion conditions (Blocken, Stathopoulos, & Carmeliet, 2007). In this study area, because the solar panels had a wide wind inlet and a narrow wind outlet, the speed of the wind flowing through the solar panels was decreased at the inlet and increased at the outlet. This change formed three distinct zones: the deflation zone (under the solar panels), an abrasion zone, and a deposition zone (between the rows of the solar panels). Deflation zones resulted in slight wind erosion on the surface layer. The abrasion zones formed severe wind erosion and caused a V-shaped trench that is typically 1 m wide and 1 m deep at the air outlet of the solar panel, where the downward directed wind from the rear of the solar panel intersects the soil at the front of the solar panel, and the shearing and abrasion effects of the wind cause a V-shaped trench to form. Deposition zones were located between the outer edge of the abrasion zone and the deflation zone under the next row of solar panels and formed in strips 6 m wide and with up to 40 cm depth of deposition. The appearance of serious abrasion and deposition taken together totally disrupted the original soil structure and increased the difficulties of natural vegetation restoration, which not only increased the local land degradation potential, but also resulted in some security issues and increased maintenance costs for the photovoltaic power station. Therefore, it is necessary to find appropriate measures to control and prevent the wind erosion.

4.2 | Treatments vary in their effects on wind erosion reduction

The keys to controlling wind erosion are to decrease the wind speed and the sand transport rate (Lv & Dong, 2012). In our study, engineering, plant, and biocrust treatments all showed beneficial erosion reduction effects that decreased the sand transport rates and the wind speeds near the surface compared with the control. Comb-pra

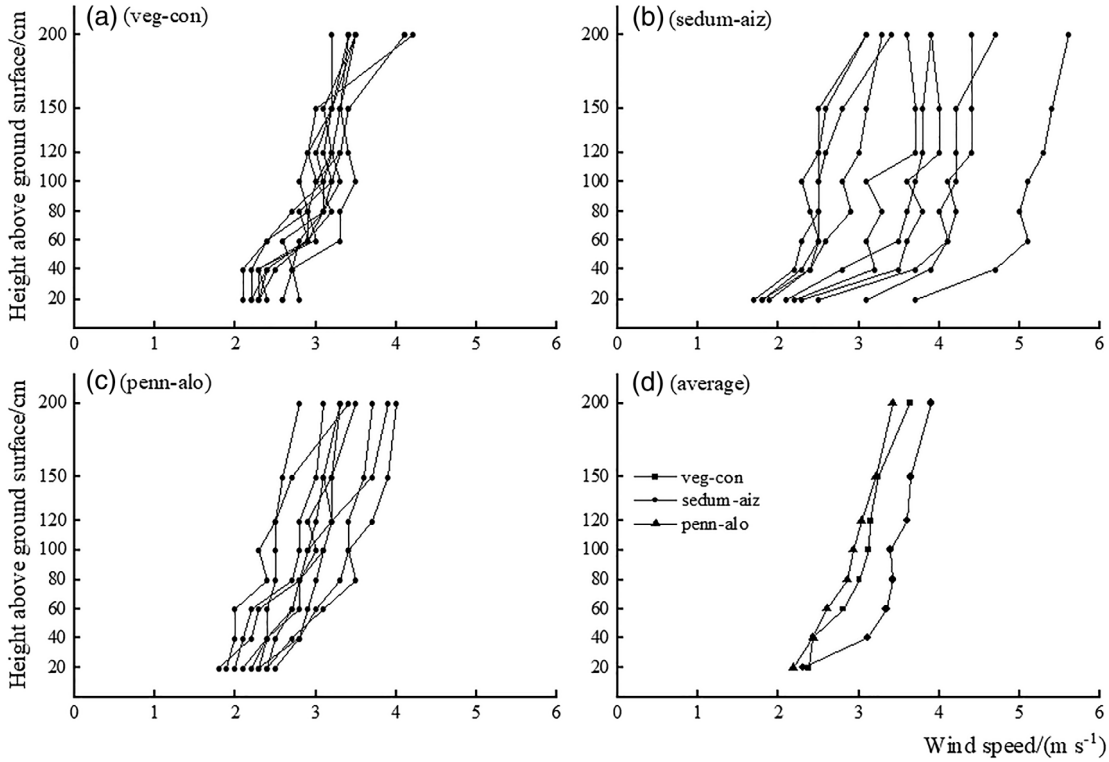

FIGURE 7 The changes in wind speed with height above the soil surface for the plant treatments where the treatments are veg-con, control treatment in plant treatments that only placed with straw checkerboard; sedum-aiz, *Sedum aizoon* L. planting area; penn-alo, *Pennisetum alopecuroides* (L.) Spreng. planting area

TABLE 3 Regression of the relationships between wind speed u_z and height z for all speed profiles under the engineering and plant treatments

Treatment		*a*	*b*	r^2	*z*0 (cm)
Engineering treatment	Bare land control	6.3157	0.8822	0.951	0.078
	Wheat straw checkerboard	3.8758	0.7918	0.911	0.748
	Gravel mulch	5.3509	0.5088	0.901	0.003
	Red clay mulch	3.1411	0.4895	0.846	0.163
	Combined measures	3.3932	0.4727	0.862	0.076
Plant treatment	Vegetation control	3.1034	0.5393	0.930	0.317
	Sedum aizoon L.	3.4918	0.6138	0.925	0.338
	Pennisetum alopecuroides (L.) Spreng.	2.9727	0.5346	0.977	0.413

and moss-crust were the optimal choices of the engineering and biocrust treatments, respectively. In the plant treatments, the sedum-aiz treatment was appropriate between the rows of the solar panels and the penn-alo treatment was appropriate in deflation zones.

4.2.1 | Engineering treatments: The comb-pra treatment performed better than other treatments

One of the most effective strategies to control wind erosion has been mulching, which reduces the direct action of wind on the soil surface (Naghizade Asl et al., 2019). In our study, all the engineering treatments had higher coverage, as compared with the control treatment, and, thus, the engineering treatments all had significant impacts on the reduction of wind erosion.

Near-surface winds are the main dynamic force causing wind erosion and strongly impact erosion by displacing or removing topsoil from the land surface (Pi & Sharratt, 2017). Therefore, the influence of the various engineering treatments on the sand transport rates was primarily concentrated within the 0–10 cm height interval above the surface. The comb-pra treatment exerted the largest reductions in the sand transport rates and had a lower sand erosion–deposit budget. Therefore, indications are that gravel application within the abrasion zones coupled with red clay applications within the deposition zones

would be a strongly preferred prevention and control practice among the engineering treatments.

Gravel mulch has been shown to change the soil hydrological processes in a manner that has resulted in increased soil nutrient contents, increased water infiltration, reduced evaporation, and increased trapping of dust particles (Li, 2003; Lv et al., 2019; Shojaei, Hakimzadeh Ardakani, Sodaiezadeh, Jafari, & Afzali, 2019). The soil water content has a significant effect on the wind's movement of soil particles, and small increases in soil moisture have been reported to cause distinct reductions in wind erosion (De Oro, Colazo, Avecilla, Buschiazzo, & Asensio, 2019; Funk, Reuter, Hoffmann, Engel, & Öttl, 2008). The abrasion zones displayed the most serious erosion losses and it is hypothesized that the higher soil water contents under the gravel mulch had more significant effects on wind erosion reductions. The gravel mulch also reduced the direct wind damage to the ground surface, which also had an important impact on reduced wind erosion. Studies have shown that when the soil surface particle fraction was <0.125 mm, the soil surface was susceptible to wind erosion (Yan et al., 2013). Although red clay is characterized by the strong bond between the soil particles, the fine particles within the surface layer were still removed easily by wind erosion. Therefore, the gravel mulch proved to be more effective than the red clay mulch within the abrasion zones. $z0$ would be expected to reach a maximum value at some critical roughness density, and $z0$ should decrease if the roughness density continued to increase, because the roughness elements would result in the physical surface becoming aerodynamically smoother (Dong et al., 2002; Nickling & Neuman, 2009). Our study exhibited similar results, as $z0$ decreased in comparison to the control treatment under the gravel-mul treatment because of the high roughness density. Combined with the decreased wind force within the deposition zones, the red clay mulch with larger values of surface roughness was more effective within this zone. Therefore, the combpra treatment exhibited improved and better wind erosion reductions compared with the single gravel-mul or the single clay-mul treatments.

Straw checkerboard has been a common preventive practice used in wind erosion control that can disrupt the rate of wind flow and reduce the speed of dune expansion (Liu & Bo, 2020; Zhang et al., 2016). The size and layout of checkerboard sand barriers have been shown to significantly affect wind erosion control (Tian et al., 2015). In the present study, the wheat straw checkerboard sand barriers had the largest $z0$ values, minimized the wind speed above the near-surface, and demonstrated significant effects on wind erosion reductions. However, because the standard installation placement of the wheat straw checkerboard having been vertically inserted 10 cm into the ground, the original soil structure was destroyed and the straw-check treatment had lower rates of wind erosion reductions in comparison to the other treatments. Therefore, the wind erosion reduction effects of the straw-check treatment were inferior to the other three treatments with the primary cause felt to be the insertion techniques commonly accepted and used during the installation of the wheat straw checkboard practices.

4.2.2 | Plant treatments: Various results exhibited within the different zones

Vegetation helped reduce wind erosion by absorption of the wind's momentum that reduced the shear stress on the surface, trapped some eroded materials, reduced the wind speed, and reduced the quantity of bare surface area (Brown, Nickling, & Gillies, 2008; Dong et al., 2000; Webb, Okin, & Brown, 2014). All these factors are closely related to the vegetation coverage; the density, types, and morphological characteristics of the vegetation; and the layout used for placement of the vegetation. The wind erosion rates increased exponentially as the vegetation coverage decreased and the wind erosion rates were markedly less when the vegetation coverage was relatively dense (Huang, Niu, Wang, Wang, & Ding, 2001; Salahat, 2016; Zhao et al., 2005). When the coverage of natural vegetation reached 60%, it has been shown that soil wind erosion was effectively prevented (Meng et al., 2018). A study of grasslands in southern Mexico indicated that herbaceous plants reduced soil erosion loss by wind and nutrient loss better than leguminous shrubs (Li et al., 2007).

In this study, both plant treatments increased the $z0$ values, consistently reduced the wind speeds within the 20-cm interval above the surface, and significantly reduced the sand transport rates, which were all factors that had significant impacts on reducing wind erosion. Particulate matter released from soils has been shown to occur as a direct result of tillage that may partially be due to a subsequent reduction in vegetable cover (Funk et al., 2008). We observed that the sand erosion deposition budgets were slightly decreased or increased within the different zones. The plausible reasons for this phenomenon may be as follows: (a) the plants grown in the deflation zone and abrasion zone played an important role in controlling and resisting wind erosion, which decreased the amounts of the sand erosion–deposit budget and/or (b) the initial plant intervention destroyed the structure and integrity of the original landforms within the deposition zone, which made the surface more vulnerable to erosion and slightly increased the amounts of the sand erosion–deposit budget. However, it is felt the phenomenon associated with the surface disruptions will gradually disappear as the growth of vegetation and the stabilization of the soil structure subsequently occur.

Sedum-aiz and penn-alo treatments showed different wind erosion reduction effects in the transport rates and the sand erosion deposition budgets within the areas between the rows of solar panels and the deflation zones. We speculated the reasons were related to the plant's morphological characteristics, the placement or layout of the vegetation, and the changed wind flow field. Plant morphology and lateral coverage have been shown to significantly affect the erosion-control characteristics of vegetation (Hong, Kim, & Im, 2016; Zhang et al., 2016; Lancaster & Baas, 2015). *S. aizoon* L. is a dicotyledon with hard stems. The stems bend less in the wind and reductions in the wind speeds typically result. This species can effectively reduce surface wind speeds within the 0–20-cm height interval and strongly influences wind speeds within the upper intervals. *P. alopecuroides* (L.) Spreng. is a monocotyledon that is susceptible to the effects of wind

and is characterized by soft stems with long and slender leaves, which are easily bent and help to protect the plant from the damage of wind erosion. In the deflation zones, the penn-alo treatment reduced the sand transport rate because a larger lateral coverage resulted from the random broadcast planting and lower wind speeds caused by the placement of the solar panels. Between the solar panels, especially within the abrasion zones that were characterized by higher wind speeds, the *P. alopecuroides* (L.) Spreng. with the soft stems were easily bent and the vegetation tended to stick to the ground, which reduced the interception efficiencies and increased the sand transport rates. The results were consistent with these observations of the vegetation properties as *P. alopecuroides* (L.) Spreng. had a higher erosion budget compared with *S. aizoon* L. within the abrasion zone (Figure 5b).

4.2.3 | Biocrust treatments: The moss-crust performed slightly better than the cyano-crust

Biocrust is a highly complex community of mosses, cyanobacteria, lichens, bacteria, etc., that initially displayed 12% coverage of the terrestrial surface, which was typical in comparison with the results of previous studies (Bu, Wu, Xie, & Zhang, 2013; Rodriguez-Caballero et al., 2018). Biocrust has been shown to have important impacts on ecosystem evolution through the maintenance of ecosystem stability by the retention of soil moisture, improvements to nutrient cycling, increased soil stability, and the reduction of water/wind erosion hazards (Bowker, Reed, Maestre, & Eldridge, 2018; Delgado-Baquerizo et al., 2016; Delgado-Baquerizo, Morillas, Maestre, & Gallardo, 2013; Ferrenberg, Faist, Howell, & Reed, 2018; Rodriguez-Caballero et al., 2018). Researchers are currently focused on desertification control using biocrusts, especially cyanobacterial crusts, that were cultured in laboratory experiments (Giraldo-Silva, Nelson, Barger, & Garcia-Pichel, 2019; Kheirfam & Roohi, 2020).

Soil properties and ground cover have been regarded as indicators of land susceptibility to wind erosion (Webb, 2020). The biocrust mulch apparently changed the physical conditions of the soil surface, increased the ground cover, and reduced the direct effects of wind erosion. Zhang, Wang, Wang, Yang, and Zhang (2006) found that in sandy soil, the wind erosion rate at a wind speed of 18 m s^{-1} with 0% crust cover was 46 times greater than when the same soil had a 90% crust cover. The exopolysaccharides are primarily composed of glucose, mannitol, arabinose, and galactose that have been secreted by biocrust bacteria in a manner that aggregates the sand particles and helps reduce the susceptibility of the larger particles to wind erosion (Kheirfam & Roohi, 2020; Zhang, 2005). It is thought that similar mechanisms were involved in this study and resulted in reduced sand transport rates, particularly within the 0–12.5 cm height above the surface. In this study, the coverage of the cyano-crust and moss-crust treatments reached approximately 60 and 70%, respectively, when fully established. The total horizontal sand transport rates observed with the cyano-crust and moss-crust treatments were significantly decreased by 65 and 71%, respectively, when compared with the control. Therefore, both biocrust treatments demonstrated effective reductions in the sand transport rates with slightly better results for the moss-crust treatment.

The wind erosion resistance exhibited by biocrusts is closely related to the crust development stage and the type and nature of surface conditions (Bu et al., 2015; Kheirfam & Asadzadeh,2020). The moss-crust was in its final successional stage for this study and would have had higher photosynthesis rates, exopolysaccharide production, biological diversity, increased soil water contents, and nutrient contents (Guo, Zhao, Zhao, Zuo, & Li, ; Housman, Powers, Collins, & Belnap, 2006; Zhang et al., 2018). These characteristics would have resulted in the moss-crust having had stronger resistance to adversity factors than the cyanobacteria was consistent with our observations. Therefore, it was concluded that the moss-crust treatment would be more appropriate for use within this area and other areas with similar environmental characteristics.

4.3 | Optimal management practices within different zones

Comparing the optimal wind erosion reduction results of the engineering, plant, and biocrusts treatments within the same areas, we found that the comb-pra treatment was more effective for use between the rows of the solar panels while moss-crust was more effective for use within the deflation zones.

Between the rows of the solar panels, both comb-pra and sedum-aiz treatments had wind erosion reduction effects; however, the comb-pra treatment was more effective when comparing the sand transport rates and the sand erosion–deposit budgets for the two treatments. This finding may be related to the erosion characteristics of the Mu Us Sandland where severe wind erosion causes significant rates of land degradation. Soil moisture contents have significant impacts on wind erosion as has been reported by many previous researchers. Increased soil moisture contents require higher wind speeds for the initial movement of soil particles and reduce the occurrence of wind erosion (De Oro et al., 2019; Sharratt & Vaddella, 2012). Therefore, wind erosion is typically more serious when the soil exists in a dry condition (Lee & Gill, 2015). In our study area, serious wind erosion primarily occurred during the spring (from March to May) and winter (from December of one year to February of the following year) seasons when there was a more or less consistent shortage of rainfall. The relatively low soil moisture contents and relatively dry soil conditions have existed within this area for extended time periods with the frequent occurrence of severe wind erosion (Wu & Ci, 2002; Zhang, Liu, Feng, Guo, & Kang, 2019). Such harsh environmental conditions have also resulted in the slow growth with small lateral and vertical coverages for the sedum-aiz treatment, which resulted in the treatment's wind erosion reduction benefits not being fully exerted during the early stages of the study (Li et al., 2007). However, the severe wind erosion occurring within the area between the rows of the solar panels and the need for the rapid establishment of erosion reduction practices as soon as possible

within our study area has led to our recommendation that the comb-pra treatment be used in these areas since this treatment offered greater coverage in a shorter time frame.

Since the Chinese government implemented the Grain for Green Project in 1999, the natural restoration of vegetation within the Mu Us Sandland has produced significant vegetative growth that has indicated this area has a relatively high vegetation carrying capacity based on the quantities of available soil water (Li, Cao, Long, Liu, & Li, 2017; Zhang & Wu, 2020). Based on visual observations for the 2–3 year period associated with all phases of this study, these translocated plants exhibited healthy growth that was dependent on natural precipitation, but also with the succession of natural vegetation, the vegetation community within the study area has shown good sustainability in beneficial and persistent growth. Therefore, in other similar areas with slight wind erosion, vegetation measures may have the same or even better erosion reduction benefits as the engineering practices, but more detailed studies should be conducted according to the actual environmental characteristics of the different regions.

Within the deflation zones, the moss-crust was a more effective management practice. Water is one of the most important limiting factors for vegetation growth in the arid and semiarid regions. Moss-crust, a typical poikilohydric plant that adapts to water conditions of the surroundings in a passive way, has strong adaptability to this environment, as the moss-crust desiccates and becomes dormant under dry conditions, and immediately begins physiological activities once wetted (Belnap, Weber, & Büdel, 2016; Grote, Belnap, Housman, & Sparks, 2010; Lange, 2003). The solar panels prevented the rainfall falling to the ground surface beneath the solar panels and reduced the soil water contents in the deflation zones. Lateral migration of the water between the rows of the solar panels and condensation water, which forms on the panels, may provide some supplemental water, and the water deficit still severely restricts the growth of *P. alopecuroides* (L.) Spreng. in this area. However, the supplemental water was sufficient to restore the physiological activity of the moss-crust. Furthermore, the arrangement of the solar panels provided a beneficial shade effect that helped promote biocrust growth and development. Combined with the strong drought resistance, the moss-crust exhibited good growth and development characteristics that played an effective role in wind erosion reduction during the 2-year observation period.

It should be noted that different regions have different environmental conditions, climatic features, geological conditions, and erosional characteristics; therefore, the selection of the most effective management practices to reduce wind erosion and help protect the ecosystems may also be different. There is a need for relevant research to be conducted to address these issues and to help protect our existing environment from the increased threat of land degradation.

5 | CONCLUSIONS

In our study, the arrangement of the solar panels changed the wind speed flow field, which produced a deflation zone (under the solar panels, slight wind erosion) and divided the area between the rows of the solar panel areas into a distinct abrasion zone (a V-shaped trench that is 1 m deep and 1 m wide) and a deposition zone (between the outer edge of the abrasion zone and the deflation zone under the next row of solar panels, which was a stripped region approximately 6 m wide and 40 cm thick). All the engineering, plant, and biocrust treatments in our study effectively reduced wind erosion. Comb-pra and moss-crust were the optimal choices of the engineering and biocrust treatments, respectively. In the engineering treatments, gravel-mul, clay-mul, and comb-pra treatments reduced the sand transport rates by 78, 74, and 87%, respectively, in comparison to the control and all produced 1–3 cm of soil deposition while the control treatment produced soil erosion. Straw-check treatment reduced the sand transport rate by 51% in comparison to the control and had the maximum $z0$ values (0.748 cm), but still produced 4–6 cm of soil erosion. The cyano-crust and moss-crust treatments in the deflation zones decreased the sand transport rates by 65 and 71%, respectively, and the sand erosion–deposit budget decreased by 109 and 114%, respectively, in comparison to the control. In plant treatments, the sedum-aiz and penn-alo treatments were well-adapted for use between the rows of the solar panel areas and within the deflation zones, respectively. The sand transport rates decreased by 20 and 36%, respectively, and increased the sand erosion–deposit budget by 40 and 22%, respectively, in comparison to the control for the sedum-aiz and penn-alo treatments within the deflation zones. Between the solar panels, the sand transport rates decreased by 86 and 78%, respectively, for the sedum-aiz and penn-alo treatments, and both plant treatments reduced the sand erosion–deposit budget. When the wind erosion reduction effects of the different practices are compared within the same areas, we recommend the establishment of the moss-crust treatment within the deflation zones, as well as the implementation of the comb-pra treatment between the rows of the solar panels.

We feel the implementation of these recommended management practices will greatly reduce the severe soil wind erosion and land degradation that is rapidly occurring at the photovoltaic power station locations on the sandy desert soils. Locations with environmental and soil conditions similar to northwest China would likely find the management practices for reducing wind erosion that are presented in this study to be beneficial in helping to stabilize the fragile ecosystems.

ACKNOWLEDGMENTS

This research was funded by the National Key Research and Development Program of China (2016YFE0203400, 2017YFC0504703), the Major Project of Collaborative Innovation of Yangling District (2017CXY-08), the National Natural Scientific Foundation of China (41971131) and the Northwest Engineering Corporation Limited of Power China Fund. Dr. Hill's salary was supported, in part, by the USDA National Institute of Food and Agriculture, Hatch Project 1014496. The authors thank the anonymous reviewers and the journal editors for their valuable comments and suggestions, and Prof. David Eldridge at the University of New South Wales who provided an independent review and significant improvements for the manuscript and his contributions are greatly appreciated.

DATA AVAILABILITY STATEMENT

The data that support the findings of this study are available from the corresponding author upon reasonable request.

ORCID

Chun Wang https://orcid.org/0000-0002-0828-8366

REFERENCES

Anderson, M., Gorley, R. N., & Clarke, K. (2008). PERMANOVA+ for primer: Guide to software and statistical methods.

Antoninka, A., Bowker, M. A., Reed, S. C., & Doherty, K. (2016). Production of greenhouse-grown biocrust mosses and associated cyanobacteria to rehabilitate dryland soil function. *Restoration Ecology*, *24*, 324–335. https://doi.org/10.1111/rec.12311

Bagnold, R. A. (1942). *The physics of blown sand and desert dunes*. Dordrecht: Springer Netherlands. https://doi.org/10.1007/978-94-009-5682-7

Belnap, J., Weber, B., & Büdel, B. (2016). Biological soil crusts as an organizing principle in drylands. In B. Weber, B. Büdel, & J. Belnap (Eds.), *Biological soil crusts: An organizing principle in drylands* (pp. 3–13). Cham: Springer International. https://doi.org/10.1007/978-3-319-30214-0_1

Blocken, B., Stathopoulos, T., & Carmeliet, J. (2007). CFD simulation of the atmospheric boundary layer: Wall function problems. *Atmospheric Environment*, *41*, 238–252. https://doi.org/10.1016/j.atmosenv.2006.08.019

Borak, J. S., Jasinski, M. F., & Crago, R. D. (2005). Time series vegetation aerodynamic roughness fields estimated from MODIS observations. *Agricultural and Forest Meteorology*, *135*, 252–268. https://doi.org/10.1016/j.agrformet.2005.12.006

Bowker, M. A., Reed, S. C., Maestre, F. T., & Eldridge, D. J. (2018). Biocrusts: The living skin of the earth. *Plant and Soil*, *429*, 1–7. https://doi.org/10.1007/s11104-018-3735-1

Brown S., Nickling W. G., & Gillies J. A. (2008). A wind tunnel examination of shear stress partitioning for an assortment of surface roughness distributions. *Journal of Geophysical Research*, *113*(F02S06), 1–13. http://dx.doi.org/10.1029/2007jf000790.

Bu, C., Wu, S., Xie, Y., & Zhang, X. (2013). The study of biological soil crusts: Hotspots and prospects. *Clean—Soil Air Water*, *41*, 899–906. https://doi.org/10.1002/clen.201100675

Bu, C., Wu, S., Yang, Y., & Zheng, M. (2014). Identification of factors influencing the restoration of Cyanobacteria-dominated biological soil crusts. *PLoS One*, *9*, e90049. https://doi.org/10.1371/journal.pone.0090049

Bu, C., Zhao, Y., Hill, R. L., Zhao, C., Yang, Y., Zhang, P., & Wu, S. (2015). Wind erosion prevention characteristics and key influencing factors of bryophytic soil crusts. *Plant and Soil*, *397*, 163–174. https://doi.org/10.1007/s11104-015-2609-z

Butterfield, G. R. (1991). Grain transport rates in steady and unsteady turbulent airflows. In O. E. Barndorff-Nielsen & B. B. Willetts (Eds.), *Aeolian grain transport* (Vol. 1, pp. 97–122). Vienna: Springer. https://doi.org/10.1007/978-3-7091-6706-9_6

Chasek, P., Akhtar-Schuster, M., Orr, B. J., Luise, A., Rakoto Ratsimba, H., & Safriel, U. (2019). Land degradation neutrality: The science-policy interface from the UNCCD to national implementation. *Environmental Science & Policy*, *92*, 182–190. https://doi.org/10.1016/j.envsci.2018.11.017

Cheng, H., He, J., Xu, X., Zou, X., Wu, Y., Liu, C., … Zhang, H. (2015). Blown sand motion within the sand-control system in the southern section of the Taklimakan Desert Highway. *Journal of Arid Land*, *7*, 599–611. https://doi.org/10.1007/s40333-015-0126-9

Chi, W., Zhao, Y., Kuang, W., & He, H. (2019). Impacts of anthropogenic land use/cover changes on soil wind erosion in China. *Science of the Total Environment*, *668*, 204–215. https://doi.org/10.1016/j.scitotenv.2019.03.015

Dai, Y., Dong, Z., Li, H., He, Y., Li, J., & Guo, J. (2019). Effects of checkerboard barriers on the distribution of aeolian sandy soil particles and soil organic carbon. *Geomorphology*, *338*, 79–87. https://doi.org/10.1016/j.geomorph.2019.04.016

De Oro, L. A., Colazo, J. C., Avecilla, F., Buschiazzo, D. E., & Asensio, C. (2019). Relative soil water content as a factor for wind erodibility in soils with different texture and aggregation. *Aeolian Research*, *37*, 25–31. https://doi.org/10.1016/j.aeolia.2019.02.001

Delgado-Baquerizo, M., Maestre, F. T., Eldridge, D. J., Bowker, M. A., Ochoa, V., Gozalo, B., … Singh, B. K. (2016). Biocrust-forming mosses mitigate the negative impacts of increasing aridity on ecosystem multifunctionality in drylands. *New Phytologist*, *209*, 1540–1552. https://doi.org/10.1111/nph.13688

Delgado-Baquerizo, M., Morillas, L., Maestre, F. T., & Gallardo, A. (2013). Biocrusts control the nitrogen dynamics and microbial functional diversity of semi-arid soils in response to nutrient additions. *Plant and Soil*, *372*, 643–654. https://doi.org/10.1007/s11104-013-1779-9

Doherty, K. D., Antoninka, A. J., Bowker, M. A., Ayuso, S. V., & Johnson, N. C. (2015). A novel approach to cultivate biocrusts for restoration and experimentation. *Ecological Restoration*, *33*, 13–16. https://doi.org/10.3368/er.33.1.13

Dong, Z., Fryrear, D., & Gao, S. (2000). Modeling the roughness effect of blown-sand-controlling standing vegetation in wind tunnel. *Journal of Desert Research*, *20*, 260–263. https://doi.org/10.3321/j.issn:1000-694X.2000.03.008

Dong, Z., Gao, S., & Fryrear, D. (2000). Drag measurement of standing vegetation—Clod cover surface. *Journal of Soil Water Conservation*, *14*, 7–11. https://doi.org/10.13870/j.cnki.stbcxb.2000.01.002

Dong, Z., Sun, H., & Zhao, A. (2004). WITSEG sampler: A segmented sand sampler for wind tunnel test. *Geomorphology*, *59*, 119–129. https://doi.org/10.1016/j.geomorph.2003.09.010

Dong, Z., Wang, H., Liu, X., Li, F., & Zhao, A. (2002). Velocity profile of a sand cloud blowing over a gravel surface. *Geomorphology*, *45*, 277–289. https://doi.org/10.1016/S0169-555X(01)00159-3

Etyemezian, V., Nikolich, G., & Gillies, J. A. (2017). Mean flow through utility scale solar facilities and preliminary insights on dust impacts. *Journal of Wind Engineering and Industrial Aerodynamics*, *162*, 45–56. https://doi.org/10.1016/j.jweia.2017.01.001

Ferrenberg, S., Faist, A. M., Howell, A., & Reed, S. C. (2018). Biocrusts enhance soil fertility and *Bromus tectorum* growth, and interact with warming to influence germination. *Plant and Soil*, *429*, 77–90. https://doi.org/10.1007/s11104-017-3525-1

Funk, R., Reuter, H. I., Hoffmann, C., Engel, W., & Öttl, D. (2008). Effect of moisture on fine dust emission from tillage operations on agricultural soils. *Earth Surface Processes and Landforms*, *33*, 1851–1863. https://doi.org/10.1002/esp.1737

Gilbey, B., Davies, J., Metternicht, G., & Magero, C. (2019). Taking land degradation neutrality from concept to practice: Early reflections on LDN target setting and planning. *Environmental Science & Policy*, *100*, 230–237. https://doi.org/10.1016/j.envsci.2019.04.007

Giménez, A., Lozano, F. J., Torres, J. A., & Asensio, C. (2019). Automated system for soil wind erosion studies. *Computers and Electronics in Agriculture*, *164*, 104889. https://doi.org/10.1016/j.compag.2019.104889

Giraldo-Silva, A., Nelson, C., Barger, N. N., & Garcia-Pichel, F. (2019). Nursing biocrusts: Isolation, cultivation, and fitness test of indigenous cyanobacteria. *Restoration Ecology*, *27*, 793–803. https://doi.org/10.1111/rec.12920

Grote, E. E., Belnap, J., Housman, D. C., & Sparks, J. P. (2010). Carbon exchange in biological soil crust communities under differential temperatures and soil water contents: Implications for global change. *Global Change Biology*, *16*, 2763–2774. https://doi.org/10.1111/j.1365-2486.2010.02201.x

Guo, Y., Zhao, H., Zhao, X., Zuo, X., & Li, Y. (2007). Study on crust development and its influences on soil physicochemical properties in Horqin Sandy Land. *Journal of Soil and Water Conservation*, *21*, 135–139. https://doi.org/10.13870/j.cnki.stbcxb.2007.01.033.

Hong, C., Chenchen, L., Xueyong, Z., Huiru, L., Liqiang, K., Bo, L., & Jifeng, L. (2020). Wind erosion rate for vegetated soil cover: A prediction model based on surface shear strength. *Catena*, *187*, 104398. https://doi.org/10.1016/j.catena.2019.104398

Hong, Y., Kim, D., & Im, S. (2016). Assessing the vegetation canopy influences on wind flow using wind tunnel experiments with artificial plants. *Journal of Earth System Science*, *125*, 499–506. https://doi.org/10.1007/s12040-016-0684-z

Housman, D. C., Powers, H. H., Collins, A. D., & Belnap, J. (2006). Carbon and nitrogen fixation differ between successional stages of biological soil crusts in the Colorado Plateau and Chihuahuan Desert. *Journal of Arid Environments*, *66*, 620–634. https://doi.org/10.1016/j.jaridenv.2005.11.014

Huang, F., Niu, H., Wang, M., Wang, Y., & Ding, G. (2001). The relationship between vegetation cover and sand transport flux at Mu Us Sandland. *Acta Geographica*, *56*, 700–710. DOI: CNKI:SUN: DLXB.0.2001-06-008. https://doi.org/10.11821/xb200106009.

Jia, H., Yong, S., & Wang, F. (1993). The soil resource in the Shenmu experimental area. *Memoir of NISWC, Academia Sinica and Ministry of Water Resources*, *2*, 36–46. http://qikan.cqvip.com/Qikan/Article/Detail?id=4001552217.

Kheirfam, H., & Asadzadeh, F. (2020). Stabilizing sand from dried-up lakebeds against wind erosion by accelerating biological soil crust development. *European Journal of Soil Biology*, *98*, 103189. https://doi.org/10.1016/j.ejsobi.2020.103189

Kheirfam, H., & Roohi, M. (2020). Accelerating the formation of biological soil crusts in the newly dried-up lakebeds using the inoculation-based technique. *Science of the Total Environment*, *706*, 136036. https://doi.org/10.1016/j.scitotenv.2019.136036

Lancaster, N., & Baas, A. (1998). Influence of vegetation cover on sand transport by wind: field studies at Owens Lake, California. *Earth Surface Processes and Landforms*, *23*(1), 69–82. https://doi.org/10.1002/(sici)1096-9837(199801)23:1<69::aid-esp823>3.0.co;2-g.

Lange, O. L. (2003). Photosynthesis of soil-crust biota as dependent on environmental factors. In J. Belnap & O. L. Lange (Eds.), *Biological soil crusts: Structure, function, and management* (pp. 217–240). Berlin and Heidelberg: Springer. https://doi.org/10.1007/978-3-642-56475-8_18

Lee, J. A., & Gill, T. E. (2015). Multiple causes of wind erosion in the Dust Bowl. *Aeolian Research*, *19*, 15–36. https://doi.org/10.1016/j.aeolia.2015.09.002

Li, J., Okin, G. S., Alvarez, L., & Epstein, H. (2007). Quantitative effects of vegetation cover on wind erosion and soil nutrient loss in a desert grassland of southern New Mexico, USA. *Biogeochemistry*, *85*, 317–332. https://doi.org/10.1007/s10533-007-9142-y

Li, J., Okin, G. S., & Epstein, H. E. (2009). Effects of enhanced wind erosion on surface soil texture and characteristics of windblown sediments. *Journal of Geophysical Research: Biogeosciences*, *114*(G2), 1–8. http://dx.doi.org/10.1029/2008jg000903.

Li, X.-Y. (2003). Gravel–sand mulch for soil and water conservation in the semiarid loess region of northwest China. *Catena*, *52*, 105–127. https://doi.org/10.1016/S0341-8162(02)00181-9

Li, Y., Cao, Z., Long, H., Liu, Y., & Li, W. (2017). Dynamic analysis of ecological environment combined with land cover and NDVI changes and implications for sustainable urban–rural development: The case of Mu Us Sandy Land, China. *Journal of Cleaner Production*, *142*, 697–715. https://doi.org/10.1016/j.jclepro.2016.09.011

Liu, J., & Kimura, R. (2018). Wind speed characteristics and blown sand flux over a gravel surface in a compact wind tunnel. *Aeolian Research*, *35*, 39–46. https://doi.org/10.1016/j.aeolia.2018.09.005

Liu, L., & Bo, T. (2020). Effects of checkerboard sand barrier belt on sand transport and dune advance. *Aeolian Research*, *42*, 100546. https://doi.org/10.1016/j.aeolia.2019.100546

Liu, X., & Dong, Z. (2003). Review of aerodynamic roughness length. *Journal of Desert Research*, *23*, 337–346. https://doi.org/10.3321/j.issn:1000-694X.2003.04.001.

Lv, P., & Dong, Z. (2012). Study of the windbreak effect of shrubs as a function of shrub cover and height. *Environmental Earth Sciences*, *66*, 1791–1795. https://doi.org/10.1007/s12665-011-1402-4

Lv, W., Qiu, Y., Xie, Z., Wang, X., Wang, Y., & Hua, C. (2019). Gravel mulching effects on soil physicochemical properties and microbial community composition in the Loess Plateau, northwestern China. *European Journal of Soil Biology*, *94*, 103115. https://doi.org/10.1016/j.ejsobi.2019.103115

Ma, R., Wang, J., Qu, J., Liu, J., Sun, T., & Wei, L. (2010). Study on protective effect of difference types of cotton haulm sand barriers. *Journal of Soil and Water Conservation*, *24*, 50–53. https://d.wanfangdata.com.cn/periodical/trqsystbcxb201002011.

Maestre, F. T., Bowker, M. A., Eldridge, D. J., Cortina, J., Lázaro, R., Gallardo, A., … Valencia, E. (2016). Biological soil crusts as a model system in ecology. In B. Weber, B. Büdel, & J. Belnap (Eds.), *Biological soil crusts: An organizing principle in drylands* (pp. 407–425). Cham: Springer International. https://doi.org/10.1007/978-3-319-30214-0_20

Meng, Z., Dang, X., Gao, Y., Ren, X., Ding, Y., & Wang, M. (2018). Interactive effects of wind speed, vegetation coverage and soil moisture in controlling wind erosion in a temperate desert steppe, Inner Mongolia of China. *Journal of Arid Land*, *10*, 534–547. https://doi.org/10.1007/s40333-018-0059-1

Ministry of Water Resources of the People's Republic of China (2018). National Bulletin of Soil and Water Conservation.

Naghizade Asl, F., Asgari, H. R., Emami, H., & Jafari, M. (2019). Combined effect of micro silica with clay, and gypsum as mulches on shear strength and wind erosion rate of sands. *International Soil and Water Conservation Research*, *7*, 388–394. https://doi.org/10.1016/j.iswcr.2019.03.003

National Energy Administration (2018). Photovoltaic power generation statistics in 2018. http://www.nea.gov.cn/2019-03/19/c_137907428.htm

Nickling, W. G., & Neuman, M. K. (2009). *Aeolian sediment transport*. Dordrecht: Springer Netherlands. https://doi.org/10.1007/978-1-4020-5719-9_17

Pacheco, F. A. L., Sanches Fernandes, L. F., Valle Junior, R. F., Valera, C. A., & Pissarra, T. C. T. (2018). Land degradation: Multiple environmental consequences and routes to neutrality. *Current Opinion in Environmental Science & Health*, *5*, 79–86. https://doi.org/10.1016/j.coesh.2018.07.002

Pi, H., & Sharratt, B. (2017). Evaluation of the RWEQ and SWEEP in simulating soil and PM10 loss from a portable wind tunnel. *Soil and Tillage Research*, *170*, 94–103. https://doi.org/10.1016/j.still.2017.03.007

Prosdocimi, M., Tarolli, P., & Cerdà, A. (2016). Mulching practices for reducing soil water erosion: A review. *Earth-Science Reviews*, *161*, 191–203. http://dx.doi.org/10.1016/j.earscirev.2016.08.006.

Rodriguez-Caballero, E., Belnap, J., Büdel, B., Crutzen, P. J., Andreae, M. O., Pöschl, U., & Weber, B. (2018). Dryland photoautotrophic soil surface communities endangered by global change. *Nature Geoscience*, *11*, 185–189. https://doi.org/10.1038/s41561-018-0072-1

Salahat, M. A. (2016). Quantification of wind erosion from some arid soils in Jordan under two different management practices. *Arabian Journal of Geosciences*, *9*, 143. https://doi.org/10.1007/s12517-015-2183-y

Sharratt, B. S., & Vaddella, V. K. (2012). Threshold friction velocity of soils within the Columbia Plateau. *Aeolian Research*, *6*, 13–20. https://doi.org/10.1016/j.aeolia.2012.06.002

Shen, Y., Zhang, C., Wang, X., Zou, X., & Kang, L. (2018). Statistical characteristics of wind erosion events in the erosion area of Northern China. *Catena*, *167*, 399–410. https://doi.org/10.1016/j.catena.2018.05.020

Shojaei, S., Hakimzadeh Ardakani, M. A., Sodaiezadeh, H., Jafari, M., & Afzali, S. F. (2019). Optimization of parameters affecting organic mulch test to control erosion. *Journal of Environmental Management*, *249*, 109414. https://doi.org/10.1016/j.jenvman.2019.109414

Solaun, K., & Cerdá, E. (2019). Climate change impacts on renewable energy generation. A review of quantitative projections. *Renewable and Sustainable Energy Reviews*, *116*, 109415. https://doi.org/10.1016/j.rser.2019.109415

Sutton, P. C., Anderson, S. J., Costanza, R., & Kubiszewski, I. (2016). The ecological economics of land degradation: Impacts on ecosystem service values. *Ecological Economics*, *129*, 182–192. https://doi.org/10.1016/j.ecolecon.2016.06.016

Tian, L., Wu, W., Zhang, D., Lu, R., & Wang, X. (2015). Characteristics of erosion and deposition of straw checkerboard barriers in alpine sandy land. *Environmental Earth Sciences*, *74*, 573–584. https://doi.org/10.1007/s12665-015-4059-6

Wang, R., Guo, Z., Chang, C., Xiao, D., & Jiang, H. (2015). Quantitative estimation of farmland soil loss by wind-erosion using improved particle-size distribution comparison method (IPSDC). *Aeolian Research*, *19*, 163–170. https://doi.org/10.1016/j.aeolia.2015.06.005

Wang, X., Zhang, Y., Zhang, W., & Han, Z. (2004). Wind tunnel experiment of biological crust effect on wind erodibility of sand surface in Gurbantünggüt Desert, Xinjiang. *Journal of Glaciology and Geocryology*, *26*(5), 632–638. https://doi.org/10.3969/j.issn.1000-0240.2004.05.019.

Webb, N. P., Kachergis, E., Miller, S. W., McCord, S. E., Bestelmeyer, B. T., Brown, J. R., … Zwicke, G. (2020). Indicators and benchmarks for wind erosion monitoring, assessment and management. *Ecological Indicators*, *110*, 105881. https://doi.org/10.1016/j.ecolind.2019.105881.

Webb, N. P., Okin, G. S., & Brown, S. (2014). The effect of roughness elements on wind erosion: The importance of surface shear stress distribution. *Journal of Geophysical Research*, *119*, 6066–6084. https://doi.org/10.1002/2014JD021491

Wu, B., & Ci, L. J. (2002). Landscape change and desertification development in the Mu Us Sandland, Northern China. *Journal of Arid Environments*, *50*, 429–444. https://doi.org/10.1006/jare.2001.0847

Wu, W., Zhang, D., Tian, L., Zhao, C., & Jia, F. (2013). Variable characteristics of wind profile of the artificial sand dune in sandy land around the Qinghai Lake. *Research of Soil and Water Conservation*, *20*, 162–167. http://d.wanfangdata.com.cn/periodical/stbcyj201306031.

Xu, D., & Li, D. (2020). Variation of wind erosion and its response to ecological programs in northern China in the period 1981–2015. *Land Use Policy*, *99*, 104871. https://doi.org/10.1016/j.landusepol.2020.104871

Yan, Y., Xin, X., Xu, X., Wang, X., Yang, G., Yan, R., & Chen, B. (2013). Quantitative effects of wind erosion on the soil texture and soil nutrients under different vegetation coverage in a semiarid steppe of northern China. *Plant and Soil*, *369*, 585–598. https://doi.org/10.1007/s11104-013-1606-3

Yang, M. Y. (1996). Studies of rough degree calculation method. *Journal of Arid Land Resources & Environment*, *10*, 55–57. http://qikan.cqvip.com/qikan/article/detail?id=2399941.

Yuan, C., Lei, T., Mao, L., Liu, H., & Wu, Y. (2009). Soil surface evaporation processes under mulches of different sized gravel. *Catena*, *78*, 117–121. https://doi.org/10.1016/j.catena.2009.03.002

Yuan, F., Zhang, Z., Bu, C., Yang, Y., & Yuan, S. (2016). Wind speed flow field and wind erosion control measures at photovoltaic power plant project area in Mu Us Land. *Journal of Desert Research*, *36*, 287–294. http://d.wanfangdata.com.cn/periodical/zgsm201602005.

Zhang, B., Zhang, Y., Li, X., & Zhang, Y. (2018). Successional changes of fungal communities along the biocrust development stages. *Biology and Fertility of Soils*, *54*, 285–294. https://doi.org/10.1007/s00374-017-1259-0

Zhang, C., Li, Q., Zhou, N., Zhang, J., Kang, L., Shen, Y., & Jia, W. (2016). Field observations of wind profiles and sand fluxes above the windward slope of a sand dune before and after the establishment of semi-buried straw checkerboard barriers. *Aeolian Research*, *20*, 59–70. https://doi.org/10.1016/j.aeolia.2015.11.003

Zhang, G., Azorin-Molina, C., Chen, D., Guijarro, J. A., Kong, F., Minola, L., … Shi, P. (2020). Variability of daily maximum wind speed across China, 1975–2016: An examination of likely causes. *Journal of Climate*, *33*, 2793–2816. https://doi.org/10.1175/JCLI-D-19-0603.1

Zhang, H., Fan, J., Cao, W., Harris, W., Li, Y., Chi, W., & Wang, S. (2018). Response of wind erosion dynamics to climate change and human activity in Inner Mongolia, China during 1990 to 2015. *Science of the Total Environment*, *639*, 1038–1050. https://doi.org/10.1016/j.scitotenv.2018.05.082

Zhang, M., & Wu, X. (2020). The rebound effects of recent vegetation restoration projects in Mu Us Sandy land of China. *Ecological Indicators*, *113*, 106228. https://doi.org/10.1016/j.ecolind.2020.106228

Zhang, P., Yin, Z., & Shang, H. (2016). Anti-wind erosion effect of plants in Kara Bailey Project Area. *Bulletin of Soil and Water Conservation*, *36*, 224–229. https://doi.org/10.13961/j.cnki.stbctb.2016.01.040

Zhang, X., Liu, S., Feng, K., Guo, Z., & Kang, W. (2019). Characteristic of precipitation in the Mu Us sandy area during 1961-2016. *Journal of Desert Research*, *39*, 141–150. http://qikan.cqvip.com/Qikan/Article/Detail?id=7100428584.

Zhang, Y. (2005). The microstructure and formation of biological soil crusts in their early developmental stage. *Chinese Science Bulletin*, *50*, 117–121. https://doi.org/10.1007/BF02897513

Zhang, Y. M., Wang, H. L., Wang, X. Q., Yang, W. K., & Zhang, D. Y. (2006). The microstructure of microbiotic crust and its influence on wind erosion for a sandy soil surface in the Gurbantunggut Desert of Northwestern China. *Geoderma*, *132*, 441–449. https://doi.org/10.1016/j.geoderma.2005.06.008

Zhao, C., Zheng, D., & He, W. (2005). Vegetation cover changes over time and its effects on resistance to wind erosion. *Acta Phytoecologica Sinica*, *29*, 68–73. https://doi.org/10.17521/cjpe.2005.0010

SUPPORTING INFORMATION

Additional supporting information may be found online in the Supporting Information section at the end of this article.

How to cite this article: Wang C, Hill RL, Bu C, et al. Evaluation of wind erosion control practices at a photovoltaic power station within a sandy area of northwest, China. *Land Degrad Dev*. 2021;32:1854–1872. https://doi.org/10.1002/ldr.3839